

**ALKALOID EXTRACT OF ACACIA CATECHU BARK AS  
GREEN INHIBITOR FOR MILD STEEL CORROSION IN  
1 M H<sub>2</sub>SO<sub>4</sub> SOLUTION**

A DISSERTATION WORK SUBMITTED  
FOR THE PARTIAL FULFILLMENT OF THE REQUIREMENTS  
FOR THE MASTER OF SCIENCE DEGREE IN CHEMISTRY

**SUBMITTED BY:**

**Name: Rajaram Karki**

**T.U. Examination Roll No.: CHE 1612/075**

**T.U. Registration No.: 5-2-37-347-2014**



**SUBMITTED TO:**

**DEPARTMENT OF CHEMISTRY**

**AMRIT CAMPUS**

**INSTITUTE OF SCIENCE AND TECHNOLOGY  
TRIBHUVAN UNIVERSITY, KATHMANDU, NEPAL**

**September, 2022**

# BOARD OF EXAMINER AND CERTIFICATE OF APPROVAL

This dissertation entitled, “**Alkaloid extract of *Acacia catechu* bark as green inhibitor for mild steel corrosion in 1 M H<sub>2</sub>SO<sub>4</sub> solution**” by **Mr. Rajaram Karki** under the supervision of Asst. Prof. Hari Bhakta Oli, Department of Chemistry, Amrit Campus, Tribhuvan University, Kathmandu, Nepal, and under the co-supervision of Asst. Prof. Dr. Deval Prasad Bhattarai, Department of Chemistry, Amrit Campus, Tribhuvan University, Kathmandu, Nepal, hereby submitted has been approved for partial fulfillment of the requirement for completion of his Master of Science (MSc.) Degree in Chemistry. This dissertation has not been submitted to any other university or institution previously for the award of a degree.

.....  
**Supervisor**

**Asst. Prof. Hari Bhakta Oli**

Department of Chemistry  
Amrit Campus,  
Tribhuvan University, Kathmandu, Nepal

.....  
**Co-Supervisor**

**Asst. Prof. Dr. Deval Prasad Bhattarai**

Department of Chemistry  
Amrit Campus,  
Tribhuvan University, Kathmandu, Nepal

.....  
**Internal Examiner**

**Asst. Prof. Sanjay Singh**

Department of Chemistry  
Amrit Campus,  
Tribhuvan University, Kathmandu, Nepal

.....  
**External Examiner**

**Prof. Dr. Amar Prasad Yadav**

Central Department of Chemistry  
Tribhuvan University, Kathmandu, Nepal

.....  
**M.Sc. Chemistry Coordinator**

**Assoc. Prof. Dr. Bhushan Shakya**

Department of Chemistry  
Amrit Campus,  
Tribhuvan University, Kathmandu, Nepal

.....  
**Head of the Department**

**Assoc. Prof. Kanchan Sharma**

Department of Chemistry  
Amrit Campus,  
Tribhuvan University, Kathmandu, Nepal

**Date: 4<sup>th</sup> September, 2022**

## LETTER OF RECOMMENDATION

This is to recommend that the dissertation work entitled, “**Alkaloid extract of *Acacia catechu* bark as green inhibitor for mild steel corrosion in 1 M H<sub>2</sub>SO<sub>4</sub> solution**” has been carried out by **Mr. Rajaram Karki** as partial fulfillment of the requirements of the Master of Science Degree in Chemistry. This is his original work and has been carried out under our guidance and supervision. To the best of our knowledge, this research work has not been submitted for any other degree in any institute.

.....

Supervisor

Asst. Prof. Hari Bhakta Oli

Department of Chemistry

Amrit Campus,

Tribhuvan University, Kathmandu, Nepal

.....

Co-Supervisor

Asst. Prof. Dr. Deval Prasad Bhattarai

Department of Chemistry

Amrit Campus,

Tribhuvan University, Kathmandu, Nepal

**Date: 25<sup>th</sup> August, 2022**

## DECLARATION

I, Rajaram Karki, hereby declare that the work entitled “**Alkaloid extract of *Acacia catechu* bark as green inhibitor for mild steel corrosion in 1 M H<sub>2</sub>SO<sub>4</sub> solution**” submitted to the Institute of Science and Technology Tribhuvan University as partial fulfillment for the requirements of Masters of Science Degree in Chemistry has been done by myself and has not been submitted earlier in part or full in this or any other form to any other university/institute, here or elsewhere for the award of any degree. All sources of information have been specifically acknowledged by reference to the authors or institutions.

.....

Rajaram Karki

Roll No.: CHEM 1612/075

Date: 25<sup>th</sup> August, 2022

## ACKNOWLEDGEMENTS

I would like to express my conscious deepest gratitude and sincere appreciation to my **supervisor Asst. Prof. Hari Bhakta Oli** and **Co-supervisor Asst. Prof. Dr. Deval Prasad Bhattarai** for their guidance and support for the completion of this research work.

I would also like to thank **Assoc. Prof. Kanchan Sharma**, Head of Department of Chemistry, Amrit Campus, and **Assoc. Prof. Dr. Bhushan Shakya**, Co-ordinator of M.Sc. program, Department of Chemistry, Amrit Campus.

I am also thankful to Prof. Dr. Amar Prasad Yadav and Asst. Prof. Anju Kumari Das for their kind help in Polarization measurement. I am very grateful to the University Grant Commission (UGC) which awarded me with the thesis support grant (**Grant no: MRS-78-79-S&T-32**)

I am also grateful to Mani Raj Budhathoki and Nanda Krishna Manandhar, who helped me provide all instruments. I accord my thanks to all teaching and administrative faculty members of the Chemistry Department, for giving kind support during the research work.

I am extremely grateful to my parents for their love, prayers, care, and sacrifices in educating and preparing me for my future. I am very much thankful to my wife for her love, understanding, and continuing support to complete this work. Also, I express thanks to my all friends.

Rajaram Karki

**25<sup>th</sup> August, 2022**

## ABSTRACT

*In situ* corrosion inhibition in acid cleaning processes by using green inhibitors is at the forefront in corrosion chemistry. Plant extracts, especially alkaloids, are known to be good corrosion inhibitors against mild steel corrosion. In this research, alkaloids extracted from *Acacia catechu* has been used as green corrosion inhibitor for mild steel corrosion in 1 M H<sub>2</sub>SO<sub>4</sub> solution. Qualitative chemical tests and FTIR measurements have been performed to confirm alkaloids in the extract. The weight loss measurement has been adopted for the study of inhibitor concentration effect as well as variation of inhibition efficiency for time and temperature. Weight loss measurement reveals the maximum efficiency of 93.96 % at 3 hrs at 28 °C. The 1000 ppm inhibitor can work up to a temperature of 48 °C with 84.39 % efficiency. The inhibition efficiency of extract has been studied by using weight loss and potentiodynamic polarization methods. Electrochemical measurement results revealed that the alkaloids act as a mixed type of inhibitor. The inhibition efficiency of 98.91 % and 98.54 % in the 1000 ppm of inhibitor concentration for as-immersed and immersed conditions, respectively has been achieved. The adsorption isotherm indicated the physical adsorption of alkaloids. Also, the spontaneous and endothermic adsorption processes have been indicated by thermodynamic parameters.

**Keywords:** *Acacia catechu*, *Green inhibitor*, *Mild steel*, *Weight loss*, *Polarization*, *thermodynamic parameters*.

## LIST OF ABBREVIATIONS

ACBA	Acacia catechu bark alkaloid
DW	Distilled water
MS	Mild steel
OCP	Open circuit potential
OM	Optical microscope
PDP	Potentiodynamic polarization
$\Theta$	Fraction of surface coverage
$C_{inh}$	Corrosion inhibitors
CR	Corrosion rate
$E_a$	Activation energy
$E_{corr}$	Corrosion potential
FTIR	Fourier transform infrared spectroscopy
$I_{corr}$	Corrosion current
SCE	Saturated calomel electrode
UV	Ultra-violet
$H^\circ$	Standard enthalpy
$S^\circ$	Standard entropy

## LIST OF TABLES

<i>Table 1: Phytochemical screening of the extract solution</i>	22
<i>Table 2: Variation of weight loss (g/cm<sup>2</sup>) with different immersion time at different concentrations of inhibitors.</i>	27
<i>Table 3: Inhibition efficiency (%) of different concentrations of inhibitor at different immersion time</i>	29
<i>Table 4: Weight loss (g/cm<sup>2</sup>) of MS immersed in different concentrations of inhibitor at different temperatures</i>	30
<i>Table 5: Inhibition efficiency (%) of the inhibitor of different concentrations on MS at different temperatures</i>	32
<i>Table 6: Activation parameters of the MS dissolution in 1 M H<sub>2</sub>SO<sub>4</sub> without and with inhibitor.</i>	37
<i>Table 7: Anodic and cathodic slope and inhibition efficiency for as-immersed sample.</i>	40
<i>Table 8: Table showing the anodic slope, cathodic slope and inhibition efficiency for 3 hours immersed sample.</i>	41



## LIST OF FIGURES

<i>Figure 1: Acacia catechu tree</i>	7
<i>Figure 2: A diagrammatic representation to show mechanism of corrosion inhibition</i>	8
<i>Figure 3: Schematic diagram of Tafel Plot</i>	10
<i>Figure 4: Google map of sample collected area</i>	17
<i>Figure 5: Schematic Chart of Methodology</i>	21
<i>Figure 6: UV-Vis spectrum of an alkaloid of Acacia catechu</i>	22
<i>Figure 7: FT-IR spectrum of alkaloid and steel immersed in 1000 ppm inhibitor for 1 hr</i>	23
<i>Figure 8: OM image of polished MS: (a) at 4x (b) at 10x (c) at 40x OM image of MS in acid: (d) at 4x (e) at 10x (f) at 40x OM image of MS in 1000 ppm inhibitor: (g) at 4x (h) at 10x (i) at 40x</i>	25
<i>Figure 9: Variation of weight loss with immersion time for the corrosion of mild steel in the solution of 1M H<sub>2</sub>SO<sub>4</sub> and solution of different inhibitor concentrations at room temperature.</i>	26
<i>Figure 10: Variation of inhibition efficiency of different inhibitor solutions in 1M H<sub>2</sub>SO<sub>4</sub> solution vs time for the corrosion of mild steel at various times.</i>	27
<i>Figure 11: Variation of weight loss versus concentration of extract on mild steel in 1 M H<sub>2</sub>SO<sub>4</sub> solution at various times.</i>	28
<i>Figure 12: Inhibition efficiency at different concentrations of inhibitor on mild steel in 1 M H<sub>2</sub>SO<sub>4</sub> solution at various times</i>	30
<i>Figure 13: Variation of weight loss of mild steel coupons in 1 M H<sub>2</sub>SO<sub>4</sub> and 200, 600, and 1000 ppm inhibitor at different temperatures.</i>	31
<i>Figure 14: Variation of inhibition efficiency with temperature on the mild steel in presence of 200, 600, and 1000 ppm inhibitor in 1 M H<sub>2</sub>SO<sub>4</sub> solution.</i>	33
<i>Figure 15: Langmuir adsorption isotherm plot for MS in 1 M H<sub>2</sub>SO<sub>4</sub> with different concentrations of inhibitor.</i>	34
<i>Figure 16: Arrhenius plot for MS in 1M H<sub>2</sub>SO<sub>4</sub> with and without inhibitor</i>	35
<i>Figure 17: Transition state plot for MS in 1M H<sub>2</sub>SO<sub>4</sub> with and without inhibitor.</i>	36
<i>Figure 18: Variation of OCP with the time of immersion of mild steel in different concentrations of inhibitor in 1M H<sub>2</sub>SO<sub>4</sub> measured at the time of immersion.</i>	38

- Figure 19: Variation of OCP with the time of immersion of mild steel in different concentrations of inhibitor in 1M H<sub>2</sub>SO<sub>4</sub> measured after 3 h immersion in solutions. 39*
- Figure 20: Potentiodynamic polarization curves for mild steel in 1M H<sub>2</sub>SO<sub>4</sub> containing different concentrations of inhibitor as-immersed condition. 39*
- Figure 21: Potentiodynamic polarization curves for mild steel in 1M H<sub>2</sub>SO<sub>4</sub> containing different concentrations of inhibitor immersed condition. 40*
- Figure 22: Inhibition efficiency of inhibitor obtained from the polarization of both immersed and as-immersed MS samples in different concentrations of inhibitor 42*

## TABLE OF CONTENTS

BOARD OF EXAMINER AND CERTIFICATE OF APPROVAL	ii
LETTER OF RECOMMENDATION	iii
DECLARATION	iv
ACKNOWLEDGEMENTS	v
ABSTRACT	vi
LIST OF ABBREVIATIONS	vii
LIST OF TABLES	viii
LIST OF FIGURES	ix
TABLE OF CONTENTS	xi
INTRODUCTION	1
1.1    Background	1
1.2    Corrosion protection methods	2
1.2.1    Design of structures	2
1.2.2    Material selection	2
1.2.3    Protective coatings	3
1.2.4    Cathodic protection	3
1.2.5    Anodic protection	3
1.2.6    Inhibitors	3
1.2.6.1    Polymer inhibitor	4
1.2.6.2    Inorganic inhibitor	4
1.2.6.3    Organic inhibitor	4
•    Synthetic inhibitors	5
•    Green inhibitors	5
1.3 <i>Acacia catechu</i> (Khayer) Alkaloid as a green corrosion inhibitor	6
1.4    Introduction of alkaloid	7
1.5    Role of alkaloid	8
1.6    Corrosion monitoring methods	8
1.6.1    Weight loss measurement	9
1.6.2    Potentiodynamic polarization method	9
1.6.3    Tafel extrapolation method	10
1.7    Objectives	11
1.7.1    General objective	11

1.7.2	Specific objectives	11
CHAPTER 2		12
LITERATURE REVIEW		12
CHAPTER 3		16
MATERIALS AND METHODS		16
3.1	Materials	16
3.1.1	Solvents and chemicals	16
3.1.2	Instruments	16
3.2	Methods for sample preparation	16
3.2.1	Collection of plant and preparation of powder	16
3.2.2	Alkaloid Extraction	17
3.2.3	Preparation of mild steel sample	17
3.2.4	Preparation of inhibitor solution	18
3.2.5	Preparation of corrosive environment	18
3.3	Tests for Alkaloids	18
3.3.1	Mayer's Test	18
3.3.2	Dragendroff's Test	18
3.3.3	Wagner's Test	18
3.4	Weight loss measurement	19
3.5	Electrochemical Measurements	19
3.5.1	Open circuit potential measurement	19
3.5.2	Potentiodynamic Polarisation	20
3.5.3	UV-Visible Spectroscopic Analysis	20
3.5.4	FTIR Analysis	20
3.5.5	Optical microscopy	21
CHAPTER 4		22
RESULTS AND DISCUSSION		22
4.1	Test of Alkaloids	22
4.2	UV Spectroscopic Measurements	22
4.3	FT-IR Analysis	23
4.4	Optical microscopy image	24
4.5	Weight Loss Measurements	25
4.5.1	Variation of weight loss with immersion time	25
4.5.2	Weight loss of MS in different concentrations of alkaloid at different time	28

4.5.3	Inhibition efficiency by different concentrations of alkaloid	28
4.5.4	Variation of weight loss with temperature	30
4.5.5	Effect of Temperature on Inhibition Efficiency	31
4.6	Adsorption Isotherm	33
4.7	Activation Energy	34
4.7.1	Enthalpy and Entropy measurement	36
4.8	Electrochemical Methods	37
4.8.1	Open circuit potential (OCP) measurement	37
4.8.2	Polarisation measurement of As - immersed MS	39
4.8.3	Polarisation measurement of 3 hrs immersed MS sample	40
4.8.4	Inhibition efficiency from polarization measurement	41
4.9	Corrosion Inhibition Mechanism	42
CHAPTER 5		45
CONCLUSION		45
References		47

# CHAPTER-1

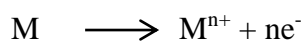
## INTRODUCTION

### 1.1 Background

The study of mild steel corrosion is important both theoretically and practically. Mild steel is utilized in the manufacturing of engineering materials, reaction tanks, vessels, and pipelines. Acid is used for cleaning, pickling, or descaling of mild steel during which, acids come into contact and is likely to cause corrosion (Ikeuba et al., 2013). Mild steel is a well-known ferrous alloy with a composition of (0.15-0.30 % C, 0.4 % Si, 0.7-0.9 % Mn, 0.04 % S, 0.04 % P, and the remainder of Fe). Mild steel is used exorbitantly as a construction material by virtue of its great mechanical qualities, ease of fabrication, excellent weldability, and low purchasing cost (Yaro et al., 2013). Corrosion occurs in mild steel, which is an unwelcome natural occurrence whose avoidance procedure is extremely difficult for the industry to complete and requires the industry to endure a significant financial expense to do so. Corrosion's current global cost is estimated to be US\$2.5 trillion, or 3.4 percent of global GDP (Koch, 2017). In the case of Nepal, it is projected that corrosion will cost the country around 4.3 % of GDP (Karki, 2021).

Corrosion occurs when metal is exposed to the corroding atmosphere. To reduce corrosion rate, methods like surface modification, coatings, galvanization, passivation, use of inhibitors, etc. are at the forefront (Pritzl et al., 2014). These methods have their own advantages and limitations. The selection and use of these methods depend on the nature of the aggressive environment. In the processes like pickling, cleaning, descaling, etc. mineral acids are heavily used. The use of acids removes the surface corrosion on the metal surface and also it offers corrosion (Gupta et al., 2020). Corrosion is a spontaneous electrochemical reaction in which anodic and cathodic processes take place. In an anodic reaction, metal/alloy dissolves due to the liberation of electrons, whereas in a cathodic reaction, ions are reduced. The most prevalent response in the mild steel dissolution process in an acidic media is as follows:

Oxidation of mild steel



Reduction of oxygen in acidic medium

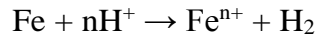


Hydrogen evolution from the acidic solution



Where M is Fe for mild steel, n is the integer that represents the number of electrons involved in the reaction.

The overall reaction is,



Replacement of corroded equipment and materials, the shutdown of electrical, chemical, and nuclear plants, pollution and loss of valuable products, substantial harm to product liability, and public safety and health are all major economic and social implications of corrosion.

## **1.2 Corrosion protection methods**

Corrosion is a natural and spontaneous process that cannot be avoided, although it can be slowed down by employing effective methods and strategies. Corrosion can be controlled in several ways. Some of the methods for corrosion control are presented below.

### **1.2.1 Design of structures**

The primary technique for corrosion control of materials, metals/alloys, composites, equipment, and infrastructure is corrosion inhibition through good design (Davis, 2000). Corrosion prevention and control must be a part of the overall design process, not an afterthought because areas where the corrosive medium becomes more corrosive (such as dead spaces or cracks) can be avoided during the design phase. In this approach, using rational design principles removes many corrosion issues while also drastically reduces the time and expense of corrosion maintenance and repair (Schouten, & Gellings, 1984).

### **1.2.2 Material selection**

Following an implementation of a correct design of material, corrosion control via proper material selection is the next step in the corrosion control process. There are many options in the choice of metals and materials each with its own intrinsic and unique corrosion behavior that can range from noble metals' (gold and platinum) excellent corrosion resistance to active metals' low corrosion resistance. Metal corrosion resistance is highly influenced by the environment such as chemical composition, temperature, velocity, and so on (Davis, 2000).

### 1.2.3 Protective coatings

The next corrosion management strategy is to coat the metal surface with a protective coating that seals it off from the environment. These coatings can be metallic, inorganic, or organic, and can be applied in a variety of ways, including dipping, spraying, electrolytic deposition, and so on (Schouten, & Gellings, 1984).

### 1.2.4 Cathodic protection

Cathodic protection is one of the most important corrosion protection techniques, in which corrosion damages are reduced to almost zero by using an externally applied electric current, and metallic substances can be kept in a corrosive environment for an indefinite time without deterioration or degradation (Boeckmann et al., 1997).

### 1.2.5 Anodic protection

The anodic protection method is based on the formation of a protective film on metals and alloys by externally applied anodic currents, and it is considered as one of the most significant advances in corrosion science because it not only protects metals and alloys but also provides a direct means of monitoring their corrosion rates (Ahmad, 2006).

### 1.2.6 Inhibitors

A corrosion inhibitor is a chemical substance that upon addition to a corrosive environment, results in the reduction of corrosion rate to an acceptable level. It has been explored the development of more reliable methods and strategies to prevent or minimize acid corrosion. The use of inhibitors is one of the most effective and successful methods for such processes in an acid medium (Jeyaprabha et al., 2006). Corrosion inhibitors are generally used in small concentrations. A corrosion inhibitor should not only mitigate corrosion but also be compatible with the environment. Usually, a corrosion inhibitor is rated in terms of inhibition efficiency (*IE*) and

$$\text{defined as, } IE = \frac{(CR)_o - (CR)_i}{(CR)_o} \times 100 \quad \dots (1)$$

Where,  $C_R$  is the corrosion rate and the subscripts *i* and *o* refer, respectively to the presence and absence of inhibitor. In the case of inhibitors that adsorb on the metal surface and inhibit the corrosion, there are two steps: (i) transport of inhibitor to the metal surface and (ii) metal–inhibitor interactions (Shastri, 2011). There are various types of inhibitors that are used according to their uses and efficiency.



### **1.2.6.1 Polymer inhibitor**

Polymeric materials are safe for the environment, non-toxic, and relatively inexpensive. Because most polymers are not easily biodegradable, they can be stored for a long time and are used to protect metals and alloys from corrosion. Most metals require a coating with a thickness of 250 to 400 nm to protect them against corrosion. As is well known, the majority of polymeric materials can withstand temperatures of up to 150 °C, and many of them can withstand temperatures of up to 40 °C to 50 °C (vinyl plant, polyisobutylene, etc.). Polyorganosiloxanes are effective at preventing corrosion. Fiberglass offers a wide range of applications in industrial plants. Epoxy resins, epoxy lacquers, and nylon have all been discovered to be quite useful in the fight against metal corrosion (Arthur et al., 2013). Umoren et al. studied the corrosion inhibition of mild steel in H<sub>2</sub>SO<sub>4</sub> in the presence of gum arabic (naturally occurring polymer) and polyethylene glycol (PEG) (synthetic polymer). It was found that PEG was more effective than gum arabic and acetyl thiourea chitosan polymer (ATUCS).

### **1.2.6.2 Inorganic inhibitor**

Many oxy-anions have been utilized as corrosion inhibitors, including dichromates, chromates, tungstates, molybdates, nitrites, and nitrates. These oxidizing anions are potent inhibitive anions. They also serve as a chelating agent and abrasive particle, among other things. Some corrosion inhibitors' efficacy is determined by the type of material, its qualities, and the corrosive environment. The inhibitory efficiency of molybdate anion, for example, increases as the oxygen concentration in the corrosion environment rises. Some of these anions have proven to be effective in a variety of corrosive environments. Molybdates, for example, have been used to prevent mild steel and cold rolling steel corrosion in simulated cooling water, as well as zinc corrosion inhibition, bacterial corrosion, and iron corrosion. Nitrates have been used to inhibit galvanized steel corrosion, aluminum corrosion, zinc corrosion in NaCl solution on pure aluminum pit initiation in HCl solution, and steel sol-gel coatings. In the presence of halide ions, chromates are an excellent corrosion inhibitor for iron and ferrous alloys (Sayin & Karakaş, 2013).

### **1.2.6.3 Organic inhibitor**

Organic compounds are used as inhibitors, occasionally, they act as cathodic, anodic, or both, cathodic and anodic inhibitors, nevertheless, as a general rule, these act

through a process of surface adsorption, designated as a film-forming. These inhibitors build up a protective hydrophobic film adsorbed molecules on the metal surface, which provides a barrier to the dissolution of the metal in the electrolyte. They must be soluble or dispersible in the medium surrounding the metal (Galio, et al., 2014). Compounds containing nitrogen, sulfur, and oxygen are reported as the most effective and efficient inhibitors (Lagren & Bentiss, 2002). The effectiveness of those compounds is due to the presence of a lone/free pair of electrons or the presence of  $\pi$ -electrons in their structure. The efficacy of the organic inhibitors depends on their capacity to replace water molecules from the metal surface and get them adsorbed. The adsorption of organic inhibitors greatly depends on the functional groups like  $-\text{NH}_2$ ,  $=\text{NH}$ ,  $-\text{N}=\text{N}-$ ,  $-\text{CHO}$ ,  $-\text{OR}$ , etc. in the inhibitor molecule (Khaled & Hackerman, 2003; Thapa et al., 2019). Inhibitors are mainly classified into synthetic and natural types.

- **Synthetic inhibitors**

Organic compounds having heteroatoms such as O, N, S, P, X, and  $\pi$ -bonds are the most effective corrosion inhibitors. Polymers have received a lot of attention recently as corrosion inhibitors due to their inherent stability and cost-effectiveness. Also, their functional groups form complexes with metal ions, and these complexes blanket the metal surface, sheltering it from corrosive chemicals present in the solution. Some research groups have investigated the use of polymers as corrosion inhibitors of metals in aggressive media. Polymers such as polyvinyl alcohol, polyethylene glycol, polyvinyl pyridine, polyvinylpyrrolidone (PVP) polyethyleneimine, polyacrylic acid, polyaniline, polyacrylamide, and polyvinyl imidazoles have been reported. Because of the presence of the  $-\text{C}=\text{N}-$  group (imines), N, and O atoms in the molecule, Schiff bases ( $\text{R}_2\text{C}=\text{NR}'$ ) are considered strong corrosion inhibitors for a variety of metal/alloy surfaces in acidic conditions (Arshad et al., 2019). The uses of synthetic inhibitors are limited due to their toxicity, expensive, and complex synthetic routes.

- **Green inhibitors**

Natural inhibitors, generally termed, green inhibitors are reported with good inhibition efficiency. So, in recent years attention has been focused on natural products such as greenery and ecofriendly inhibitors (Gupta et al., 2020; Shrestha et al., 2019). Natural products with high molecular weight and bulky hetero functional

moieties like alkaloid, flavonoid, amino acids, glucose, saponins, tannins, etc. are being used for corrosion inhibition processes (Finšgar & Jackson, 2014; Rahim et al., 1997). Green corrosion inhibitors can either be scavengers or interface inhibitors. Scavengers lower medium corrosivity by scavenging aggressive chemicals, whereas interface inhibitors prevent corrosion at the metal-environment contact by forming a coating. The availability of organic compounds with N, O, P, and S atoms that have a shielding effect and corrosion-inhibiting potential for the material attack has been connected to the corrosion inhibition efficacy of organic green corrosion inhibitors (OGCIs) (Yildirim and Cetin, 2008). Their increasing order of corrosion inhibition efficiency has been stated to be oxygen < nitrogen < sulfur < phosphorus (Neha et al., 2013). OGCI exhibit their inhibiting action via physisorption or chemisorption onto the metal-solution interface by removing molecules of water on the surface for compact barrier film formation (Finšgar and Jackson, 2014). The occurrence of a coordinate covalent bond by the interaction between lone pair and  $\pi$ -electrons available in the molecules of OGCI with the vacant metal  $d$ -orbitals is also experienced (Abdallah, 2002). Nevertheless, compound adsorption on the metal surface is enhanced by  $p$ - $d$  bond formation as a result of  $p$ -electron overlap to the  $3d$  vacant orbital of the Fe atom (Ahamad et al., 2010) due to the availability of N, O, and S atoms and organic structure double bonds (Hong et al., 2008). The high focus on natural products for inhibitors is due to their biodegradable, non-toxic, inexpensive, readily available, renewable, and eco-friendly properties (Sivakumar & Srikanth, 2017).

### **1.3 *Acacia catechu* (Khayer) Alkaloid as a green corrosion inhibitor**

*Acacia catechu* is commonly known as the Cutch tree and Khair in Nepali which is a 9–12 m tall tree. This tree is deciduous and has short-snared spines which are mainly distributed all over terai and hilly region at a altitude upto 1500 m. It is a useful multi-purpose tree producing fuel, wood, small timber, and fodder which is very popular among the local people in the Terai region. The systematic classification of the plant is given below.

Kingdom	-	Plantae
Subkingdom	-	Viridiplantae
Infrakingdom	-	Streptophyta
Superdivision	-	Embryophyta
Division	-	Tracheophyta
Subdivision	-	Spermatophytina
Class	-	Magnoliopsida
Superorder	-	Rosanae
Order	-	Fabales
Family	-	Fabaceae
Genus	-	<i>Acacia</i>
Species	-	<i>catechu</i>
Vernacular name	-	Khair



Figure 1: *Acacia catechu* tree

*Acacia catechu* is commonly used in Ayurveda to cure a variety of ailments. Asthma, cough, bronchitis, colic, diarrhea, dysentery, boils, skin ailments, ulcers, and stomatitis are all treated with its heartwood extract. In the southern portion of India, heartwood decoction is consumed as a beverage (Sunil et al., 2019). The most important commercial product from *Acacia Catechu* is Kathha and Cutch. Katha is mainly used for chewing with betel nut and paan, whereas the bi-product cutch is used in tanning and dyeing ships. The prime focus of this research is to analyze the efficiency of alkaloids from bark extract as a green inhibitor on the surface of mild steel.

Catechin, epicatechin, gallate, procatechuic acid, tannins, alkaloids quercetin, and kaempferol are some of the most important phytoconstituents found in *Acacia catechu*. Afzelechin gum and Porifera sterol glucosides are also detected in small amounts (Hashmat et al., 2013) in *Acacia catechu*.

#### 1.4 Introduction of alkaloid

Alkaloids are a group of naturally occurring organic compounds that contain at least nitrogen as hetero-element in the structure. They are commonly found in plants. Many alkaloids are useful therapeutic substances that can be used to treat a variety of ailments such as malaria, diabetes, cancer, and heart dysfunction (Ain, et al., 2016). Amino acids like phenylalanine, tyrosine, tryptophan, ornithine, and lysine are used

to synthesize most alkaloids. Alkaloids may contain oxygen, sulfur, and, more rarely, additional elements like chlorine, bromine, and phosphorus, in addition. Most alkaloids are colorless, non-volatile, crystalline solids with a bitter taste in their pure form. Morphine, codeine, coniine, quinine, scopolamine, hyoscamine, atropine, caffeine, sanguinarine, berberine, etc. are examples of alkaloids (Singh, et al., 2017).

### 1.5 Role of alkaloid

Alkaloids have a wide range of physiological effects in both animals and humans. The majority of them are sourced from plants (Verma, et al., 2019). Because of their natural and biological origins, alkaloids are considered environmentally friendly corrosion inhibitors that can replace traditional and hazardous synthetic corrosion inhibitors. In various electrolytic media, a variety of alkaloids have been used as effective corrosion inhibitors for metals and alloys. Alkaloid molecules have been shown to have substantial conjugation in the form of non-bonding and  $\pi$ -elections, allowing them to interact robustly and effectively block corrosion (Verma, et al., 2019).

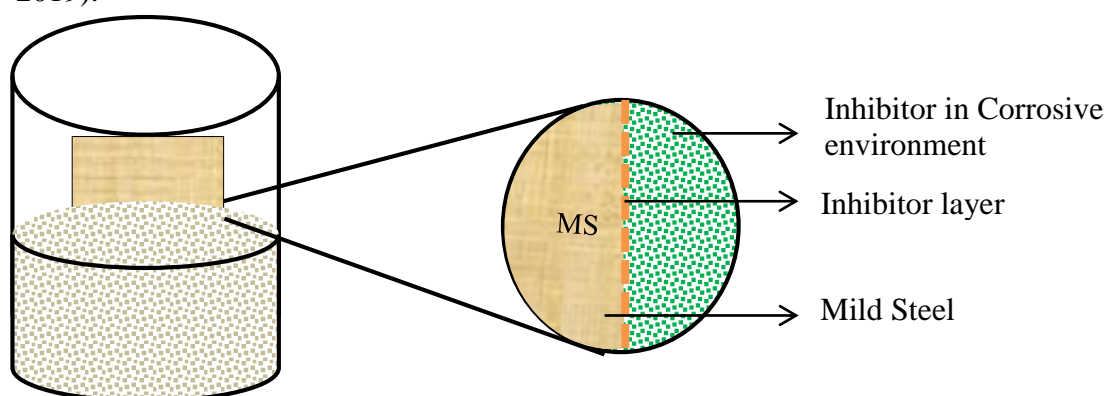


Figure 2: A diagrammatic representation to show mechanism of corrosion inhibition

### 1.6 Corrosion monitoring methods

Corrosion monitoring is the quantitative measure of the changes in material over time, such as weight loss, changes in physical, chemical, electrical, magnetic, or mechanical characteristics, and component integrity loss, among other things (Kansara, et al., 2018). The qualities of metal, the environment, and the metal-environment interface are used in corrosion monitoring systems since these are the primary influences on corrosion. Corrosion monitoring techniques can provide a wealth of data and information that can be used to help with corrosion control. Corrosion monitoring techniques are divided into two categories: direct and indirect. Based on the idea that underpins them, these two are subdivided into several titles

(Shastri, 1998). Weight loss measurement, open circuit potential measurement, and potentiodynamic polarization are all employed in this experiment.

### 1.6.1 Weight loss measurement

This is the simplest and best-known method for corrosion monitoring. In this method, a small sample specimen is exposed to a corrosive environment for a specific period and subsequently removed it for the weight loss measurement. A similar experiment is repeated for the next specimen to the environment in presence of an inhibitor in similar conditions to calculate the inhibition efficiency. The corrosion rate is calculated by using the following formula,

$$\text{Corrosion rate } (v) = \frac{87600 \times \Delta W}{\rho \times A \times T} \quad \dots (2)$$

Where,  $\Delta W$  = weight loss in gram

$A$  = area in  $\text{cm}^2$

$\rho$  = density in  $\text{g/cm}^3$

$T$  = Time in hours

$$\text{Inhibition efficiency is calculated by } (IE\%) = \frac{\Delta W_a - \Delta W_p}{\Delta W_a} \times 100 \quad \dots (3)$$

Where,  $\Delta W_a$  = Weight loss in absence of an inhibitor

$\Delta W_p$  = Weight loss in presence of an inhibitor

$$\text{MS surface coverage by inhibitor molecule } (\theta) = \frac{\Delta W_a - \Delta W_p}{\Delta W_a} \quad \dots (4)$$

### 1.6.2 Potentiodynamic polarization method

Potentiodynamic polarization (PDP) is a method that involves applying a current through the electrolyte to change the electrode's potential at a set pace. In corrosion testing, this procedure is used to polarize specimens. One of the most often utilized DC electrochemical methods in corrosion measurements is PDPs. In PDPs, a wide range of potentials is given to the test electrode, causing a dominating oxidation or reduction process on the metal surface (depending on the direction of polarization) and, as a consequence, an appropriate current to be produced. The polarization curve is obtained by plotting the potential as a function of current density at each measured point. The polarization curve may be used to calculate the metal's corrosion potential and rate under any given circumstance (Tafel slope). The advantage of this method is reflected in the possibility of localized corrosion detection, easy and quick determination of the corrosion rate, corrosion protection efficiency, and so on

(Telegdi et al., 2018). The formula to calculate the corrosion efficiency is given by the formula,

$$\text{Corrosion inhibition efficiency (\%)} = \frac{I_{\text{corr}} - I_{\text{corr}}^*}{I_{\text{corr}}} \times 100\% \quad \dots (5)$$

Where,  $I_{\text{corr}}$  = corrosion current in absence of inhibitor

$I_{\text{corr}}^*$  = corrosion current in the presence of inhibitor.

The linear Tafel segment of the anodic and cathodic curves could be extrapolated to corrosion potential to obtain corrosion current densities.

### 1.6.3 Tafel extrapolation method

Tafel extrapolation is one of the quicker experimental procedures routinely used to determine corrosion rates. The mixed potential theory underpins this strategy. Both anodic and cathodic reactions are components of a mixed electrode that participates in the corrosion process, and the location where they intersect correlates to corrosion-current density ( $I_{\text{corr}}$ ) and corrosion potential ( $E_{\text{corr}}$ ). The corrosion rate may be determined by plotting the logarithms of current density ( $\log I$  against potential and extrapolating the current densities in the two Tafel areas (Reive, 2008).

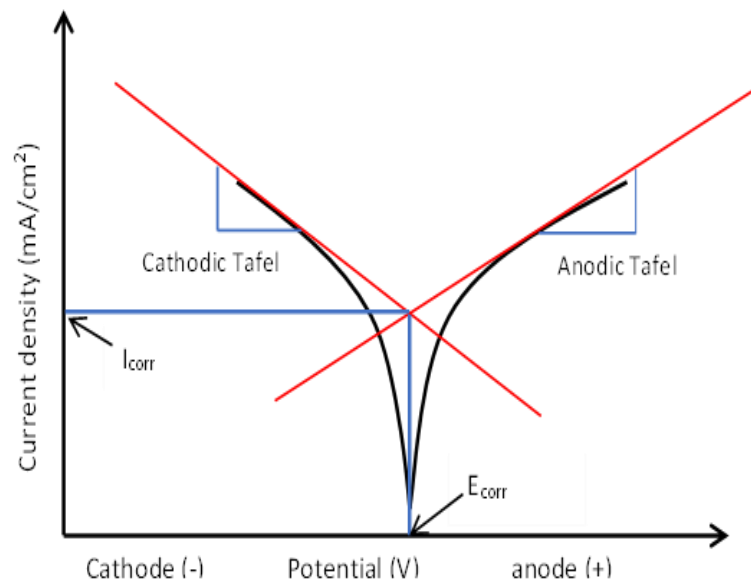


Figure 3: Schematic diagram of Tafel Plot

## **1.7 Objectives**

### **1.7.1 General objective**

The general objective of the study is extraction and characterization of alkaloids from *Acacia catechu* bark and study its anticorrosion activity.

### **1.7.2 Specific objectives**

- ❖ Extraction of alkaloid from *Acacia catechu* bark.
- ❖ Characterization of alkaloids by qualitative chemical test and spectroscopic test.
- ❖ Study of corrosion inhibition efficiency by weight loss and potentiodynamic polarization method.
- ❖ Study of various thermodynamic parameters and examination of Langmuir adsorption isotherm.



## CHAPTER 2

### LITERATURE REVIEW

Many varieties of plants are reported to behave as effective green corrosion inhibitors in an acidic environment. Some of them were examined as part of this thesis project, and the results are listed below.

Using the mass loss technique, polarization measurements, and electrochemical impedance spectroscopy at room temperature, the corrosion inhibiting efficacy of *Schreabera swietenoids* plant leaves extracts on mild steel in 1 N HCl has been investigated by Sivakumar & Srikanth (2017). The plant extracts from *Schreabera swietenoids* acted as a mixed-type inhibitor in polarization investigations. The addition of extracts improves charge transfer resistance, which enhances inhibition efficiency, according to the Nyquist plot. Photochemical components and organic moieties deposited on the metal surface were also discovered to be responsible for the inhibitor's effectiveness, as evidenced by FTIR tests. SEM image revealed the formation of a protective coating of inhibitor over the material against corrosion.

Gupta et al., (2020) studied the corrosion inhibition characteristics of methanol extract of *Jatropha curcas* (JC) for mild steel (MS) in acidic media using weight loss and potentiodynamic techniques. In the absence and presence of different quantities of the methanolic extract of *Jatropha curcas* barks, corrosion inhibition of MS in 1 M H<sub>2</sub>SO<sub>4</sub> was investigated. The results indicated the increased corrosion inhibition with the increased concentration of extract. After 24 hours in the acidic solution, the inhibitory effects of 1000 ppm JC extract from the weight loss and potentiodynamic polarization techniques were around 92.0 %. The JC extract operates as a mixed type inhibitor, according to open circuit potential (OCP) and potentiodynamic polarization studies.

Ikeuba et al., (2013) studied the effects of ethanolic (EEGK), alkaloid ethanolic (AEGK), and non-alkaloid ethanolic (NEGK) extracts of *Garcinia kola* seeds on mild steel corrosion in the sulphuric acid medium. The pertinent reactions were studied in terms of quantitative estimation of hydrogen evolution (by gasometric assembly) and weight loss techniques at 307-373 K. The extracts were shown to prevent mild steel corrosion to varying degrees in the sequence of AEGK > EEGK > NEGK. Upon increasing the inhibitor concentration and decreasing the temperature, the inhibition effectiveness was found to be improved. The pattern of inhibitory efficiency with

temperature,  $E_a$ , and  $G_{ads}$  values suggested a phenomenon of physical adsorption for the inhibition process and the process followed the Langmuir adsorption isotherm. The best inhibition efficiency was concluded on the alkaloid ethanolic extract.

The inhibitory effect of *Neolamarckia cadamba* crude extract (bark, leaves) and pure alkaloid (3b-iso-dihydro cadambine) on mild steel corrosion was examined by Raja et al., (2013) in one molar hydrochloric acid media. This research used potentiodynamic polarization, electrochemical impedance, scanning electron microscopy, FTIR spectroscopy, and molecular modeling. The corrosion rate was greatly reduced by crude extracts and 3b-iso-dihydro cadambine at all doses, according to the results. Base on the polarization measurements, these green inhibitors functioned through mixed-type inhibition. SEM tests revealed the creation of a protective film over the metal surface, while FTIR and chemical modeling confirmed that alkaloids, specifically 3b-iso-dihydro cadambine, were responsible for the shielding action.

The corrosion protection of mild steel in 1 M  $H_3PO_4$  solution by apricot juice was studied (Yaro et al., 2013) at different temperatures by weight loss technique. This research focused on adsorption, activation, and statistical analysis. According to the Langmuir isotherm, the inhibitor adsorbs on the metal surface. The average heat of adsorption on the metal surface was 14.93 kJ/mol, indicating spontaneous physical adsorption. With the addition of the inhibitor, the activation parameters did not change, indicating that the response mechanism has not changed. Temperature, inhibitor concentration, and their combined interactions all impacted the corrosion rate, according to this study.

Thapa et al., (2019) found a significant corrosion inhibition while using bark-extract of *Euphorbia royleana* in 1 M HCl solution. The significant inhibition was in 100% extract concentration and the inhibition efficiency was very poor at a higher temperature. Shrestha et al., (2019) have studied methanol extract of barks of *Lantana camara* in 1 M hydrochloric acid as a corrosion inhibitor. The inhibition efficiency is reported very high even at 200 ppm concentration of inhibitor but the inhibition at higher temperatures is very poor. Kamal & Sethuraman, (2012) studied the effect of bis- Indole alkaloid of a *Caulerpa racemosa* as a green inhibitor for the corrosion of mild steel in 1 M HCl and found the maximum efficiency at 100 ppm at 30 °C. Similarly, the corrosion alkaloid extract of *Rhynchosytilis retusa* (Chapagain et al., 2022), *Artemesia vulgaris* and *Solanum tuberosum* (Oli, 2021) has shown satisfactory corrosion inhibitions. The inhibitor from *Artemesia vulgaris* was found to be more

than 80 % efficient up to 45 °C and from remaining was found to be 70 % only at 25 °C (Oli et al., 2021).

Such many inhibitors are reported with good inhibition efficiency only below 45 °C. Plant abundance, extract with higher inhibition efficiency, and good inhibition at higher temperatures are still to be considered. In previous work, the use of the aqueous extract of *Acacia catechu* bark as a green corrosion inhibitor in mild steel has been reported (Haldhar et al., 2020). The use of aqueous extract of *Acacia catechu* (*A.catechu*) bark as a green corrosion inhibitor in MS showed its best corrosion resistance of 93.85 % at a concentration of 600 mg/L in a 0.5 M H<sub>2</sub>SO<sub>4</sub>. The aqueous extract contains only polar group-containing phytochemicals. Therefore, the efficiency of such phytochemicals is not high. The methanolic and aqueous extracts from *A. catechu* has been used as inhibitor but the alkaloid extract and its use as an inhibitor has not been carried out. In all the above-mentioned literature, there is about 80% efficiency below 45 °C temperature with immersion time less than 24 h. The efficiency of the inhibitor for prolonged immersion is to be measured. In this study, the alkaloid extract will be collected and used as an inhibitor which will have higher efficiency and can be used at a higher temperature too.

## **2.1 Research Gap**

Any material degradation can result into the shutdown of entire system resulting into the loss of production, system reputation, money, and costs in terms of environmental harm and human safety. Corrosion losses are mostly occurred in chemical, petrochemical, construction, industrial, and transportation sectors. Corrosion causes significant losses and inhibits economic progress in all nations. Corrosion costs are estimated to be around 3-4 % of the Gross National Product (GNP) in most industrialized nations of which 30-35 percent may be avoided by using corrosion prevention techniques (Koch, et al., 2016). Corrosion causes roughly 4.3 % of GDP loss in Nepal (Karki, 2021). It results in both direct and indirect losses to the economy. As a result, corrosion is regarded as one of our society's most critical issues. In this context, it is inevitable to investigate and deploy corrosion monitoring and controlling strategies.

The use of mineral acids in acid cleaning processes can lead to the corrosion of material. To minimize the corrosion during such processes, various inhibitors are

reported to use. Among these, the use of plant extract as an inhibitor with very promising efficiency has been reported. Uses of green inhibitor has been a promising technique in the field of corrosion control. However, low inhibition efficacy of green corrosion inhibitor at higher temperature even at 100 % inhibitor concentration has necessitated the study of corrosion inhibition mechanism and means of enhancing the efficacy. These limitations can be minimized by selecting suitable phytochemicals. Phytochemical constituents vary from one part of the plant to the other part of the plant as well as from one plant to another plant. In this research, the qualitative aspect of phytochemical constituents will be studied from the bark of *Acacia catechu*. Later on, the corrosion inhibition efficacy of bark-extract-alkaloid of *Acacia catechu* on mild steel in one molar sulphuric acid medium will be studied.

## CHAPTER 3

### MATERIALS AND METHODS

#### 3.1 Materials

##### 3.1.1 Solvents and chemicals

Methanol (Thermo fischer Scientific India Pvt., Ltd, Molecular weight: 32.04, specific gravity: 0.792 and percentage purity: 99%), hexane (Thermo Fischer Scientific India Pvt. Ltd., Percentage purity: 98.88 %, specific gravity: 0.667), sulphuric acid (sp. gravity 1.835, 97 % purity) were used as solvents. Deionized water (conductivity of 15micro siemens/cm, ferric chloride, conc. Hydrochloric acid, Dragendorff's reagent, conc. Nitric acid, Fehling solution, sodium hydroxide (Merc Life science, Mol. Wt.: 40, purity: 97 %), ethanol, silicon carbide sheets (100, 200, 400, 600, 800, 1000, 1200 grit) were used. Chemicals were used as received without further purification.

##### 3.1.2 Instruments

- Grinder (AMEET)
- Weighing balance (PHOENIX)
- Funnel
- Beakers and conical flask
- Double beam UV-Vis spectrophotometer (Labtronics LT-2802)
- FTIR (PerkinElmer Spectrum IR; Version 10.6.2)
- Rotatory evaporator (IKA RV 10)
- Desiccator
- Digital Vernier caliper
- Hokuto Denko potentiostat (HA151, Japan)
- Optical microscopy (Model: RXLT-4, Radical Scientific, India)

#### 3.2 Methods for sample preparation

##### 3.2.1 Collection of plant and preparation of powder

Bark portion of *Acacia catechu* was used. The plant was selected as per abundance and availability in the local area which is not listed as an endangered species. The bark of

the plant *Acacia catechu* was selected as it was not previously studied on alkaloid extract. The plant was collected from the Letang (Latitude: **26.75**, Longitude: **87.48**, and altitude **850** m), Morang district of Nepal. The collected sample was shade dried, and dry bark was ground into the fine powder with the help of a grinding machine and fine powder was taken for the extraction of alkaloid.

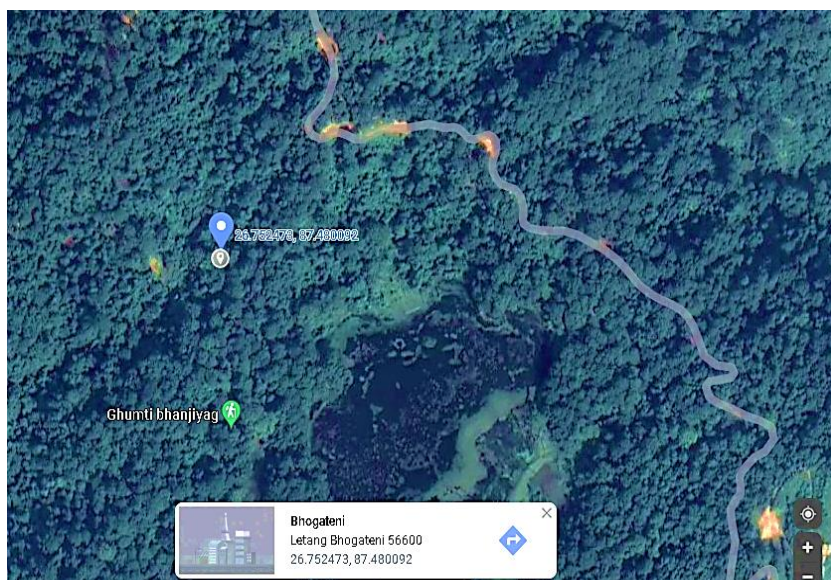


Figure 4: Google map of sample collected area

### 3.2.2 Alkaloid Extraction

100 g of powdered plant sample was soaked in hexane for 24 hrs to remove unsaturated organic compounds and fats and then filtered. The residue was taken into a glass jar and about 500 mL of methanol was poured into it. The sample was kept for about 5 days to extract phytochemicals properly and filtered until the filtrate was colorless. The filtrate was put into a big container and acidified with 5% tartaric acid and then filtered. Ammonia was added to deprotonate 1°, 2°, and 3° alkaloids, and the pH was maintained at >10. Using a separating funnel, alkaloids were extracted from this alkaline solution using chloroform. The alkaloids-containing chloroform layer was recovered in a beaker. It was first concentrated using an IKA RV 10 digital rotatory evaporator, then dried in a water bath to get a solid residue containing *Acacia catechu* alkaloid. The dry alkaloid was kept in a moisture-free desiccator in the vessel.

### 3.2.3 Preparation of mild steel sample

Mild steel sample coupons of similar dimensions (4 cm × 4 cm × 0.15 cm) were obtained from Teku, Kathmandu. Each coupon was polished using a variety of silicon

carbide sheets (100, 200, 400, 600, 800, 1000, 1200) and rinsed with hexane. Before each weight loss and electrochemical experiment, coupons are sonicated in ethanol for 30 minutes and then dried.

#### **3.2.4 Preparation of inhibitor solution**

1 g of alkaloid was dissolved in 100 mL of 1 M H<sub>2</sub>SO<sub>4</sub> to make the inhibitor stock solution. The undissolved component of the mixture was filtered off, and the filtrate was transferred to a 1000 mL volumetric flask, where 1 M H<sub>2</sub>SO<sub>4</sub> was added up to the mark. As a consequence, a stock solution of 1000 ppm was formed. By serial dilution, inhibitor solutions with concentrations of 200, 400, 600, and 800 ppm were prepared.

#### **3.2.5 Preparation of corrosive environment**

A corrosive environment was prepared by mixing 110.5 mL of conc. sulphuric acid (sp. gravity 1.835, 97 % purity) with distilled water in a 2000 mL volumetric flask. Then the solution was diluted by adding distilled water up to the mark. This solution is utilized as a corrosive medium for assessing weight loss and polarization measurements.

### **3.3 Tests for Alkaloids**

#### **3.3.1 Mayer's Test**

A small amount of extract was treated with Mayer's reagent (1.3 g of HgCl<sub>2</sub> and 5 g of KI in 100 mL distilled water). An orange precipitate of potassium-alkaloid indicates the presence of alkaloids.

#### **3.3.2 Dragendorff's Test**

A small amount of extract was treated with Dragendorff's reagent (3 g of Bismuth nitrate in 8 mL of 4 N sulphuric acid in one beaker and 12 g potassium iodide in 18 mL distilled water in another beaker followed by mixing to give an orange-red colored solution). The appearance of an orange-red precipitate of potassium-alkaloid indicates the presence of alkaloids.

#### **3.3.3 Wagner's Test**

A few drops of the extract were treated with Wagner's reagent (2 g of iodine and 6 g of KI in 100 mL of distilled water). The reddish-brown precipitate of potassium-alkaloid was formed which indicates the presence of alkaloids.

### 3.4 Weight loss measurement

The impact of immersion duration, the effect of inhibitor concentration on corrosive media, and the influence of temperature were investigated in the weight loss measurement. The dimensions of coupons were measured with a digital Vernier caliper and weighed with an electronic balance (PH2204C) before each effect was studied. The weights of the coupons were recorded before they were dipped in 100 mL of caustic medium and inhibitor solutions of various concentrations. Coupons were removed from the solution after 30 minutes, rinsed with distilled water, and dried. The weight of dry coupons was measured again to know the loss in weight. The corrosion rate was calculated using the difference in weight of the coupon before and after immersion. A similar procedure was carried out for a different immersion interval (0.5, 1, 3, 6, and 24 hrs.). Similarly, the effect of inhibitor concentration was investigated by immersing corrosion-free coupons in acid and inhibitor solutions of various concentrations (200, 400, 600, 800, and 1000 ppm) for 6 hours at room temperature (15 °C) separately. The coupons were submerged in acid and 200, 600, and 1000 ppm inhibitor solution individually for 1 hour at various temperatures (28, 38, 48, and 58 °C) to evaluate the temperature impact.

The corrosion rate (mm/y), inhibitor efficiency (IE percent), and surface coverage ( $\Theta$ ) are computed from the weight loss data using the following relation.

$$\text{Corrosion rate } (v) = \frac{87600 \times \Delta W}{\rho \times A \times T}$$

$$\text{Inhibition efficiency } (IE\%) = \frac{\Delta W_a - \Delta W_p}{\Delta W_a} \times 100$$

$$\text{Surface coverage by inhibitor molecule } (\theta) = \frac{\Delta W_a - \Delta W_p}{\Delta W_a}$$

### 3.5 Electrochemical Measurements

#### 3.5.1 Open circuit potential measurement

The open-circuit potential (OCP) is crucial for understanding how the inhibitor solution inhibits the cell. The purpose of the OCP measurement was to get a better knowledge of the mild steel sheet corrosion behavior in 1 M H<sub>2</sub>SO<sub>4</sub> solution at room temperature in the absence and presence of alkaloids as a corrosion inhibitor. The experiment was conducted in the APY Laboratory, Central Department of Chemistry, Tribhuvan University, Nepal, using a Hokuto Denko potentiostat (HA151, Japan).



The mild steel coupon was used as a working electrode, graphite was employed as a counter electrode, and a saturated calomel electrode was used as a reference electrode in a three-electrode system. For 30 minutes, the OCP was measured in different doses of inhibitor solutions for 3 hours of immersed samples.

### **3.5.2 Potentiodynamic Polarisation**

The corrosion current, corrosion potential, and Tafel slopes were all evaluated using the polarization measurement method. In the central Department of Chemistry, Tribhuvan University, Nepal, potentiodynamic polarization measurements were performed using a Hokuto Denko potentiostat (HA-151). The polarization was done with a three-electrode cell setup. The experiment was conducted in the same electrolytic cell that was used to measure the OCP. The working electrode, a mild steel specimen with a smaller area exposed in extract solution than the counter electrode was used to apply a consistent voltage to the working electrode. To link the working electrode to the SCE, a salt bridge was used. To achieve the constant OCP, each experiment was performed for 30 mins before polarization. The sample was then polarized cathodically and anodically in the potential range of -0.9 (V) to -0.1 (V), i.e.  $\pm 350$  mV from OCP. Polarization measurements were performed on steel samples in various inhibitor doses as well as in acid solution under 3 h immersed circumstances. Tafel slope, corrosion potential, and corrosion current were computed using the polarization curves. Using the formula in equation (4), the corrosion inhibition efficiency was computed. To calculate corrosion current densities, the linear Tafel segments of the anodic and cathodic curves were extrapolated to corrosion potential.

### **3.5.3 UV-Visible Spectroscopic Analysis**

The spectroscopic characterization of *Acacia catechu* alkaloids was carried out in the Department of Chemistry, Amrit Campus, Kathmandu, using a Labtronics LT-2802 double beam ultraviolet-visible (UV-Vis) spectrometer to identify unsaturation and electron-rich centers in the alkaloids. Aqueous and methanol solutions of the alkaloid were employed to record spectra.

### **3.5.4 FTIR Analysis**

The FTIR spectroscopic examination is a potent instrument for determining the kind of bonding in organic molecules, notably the functional group. The FTIR spectra of

the alkaloid sample and the immersed steel coupons in acid and 1000 ppm inhibitor were acquired in Amrit Campus, Kathmandu, using a (PerkinElmer Spectrum IR; Version 10.6.2) FTIR spectrometer. The functional groups,  $\pi$ -bond conjugate system, and aromatic and aliphatic structures present in the alkaloid samples can be determined using FTIR spectra.

### 3.5.5 Optical microscopy

It is used to take the image of the steel coupons in the microscopic range. The images were taken for steel coupons immersed in acid and 1000 ppm inhibitor solution for 1 h in different magnification scales in the Central Department of Chemistry, Tribhuvan University, Nepal using optical microscopy (Model: RXLT-4, Radical Scientific, India).

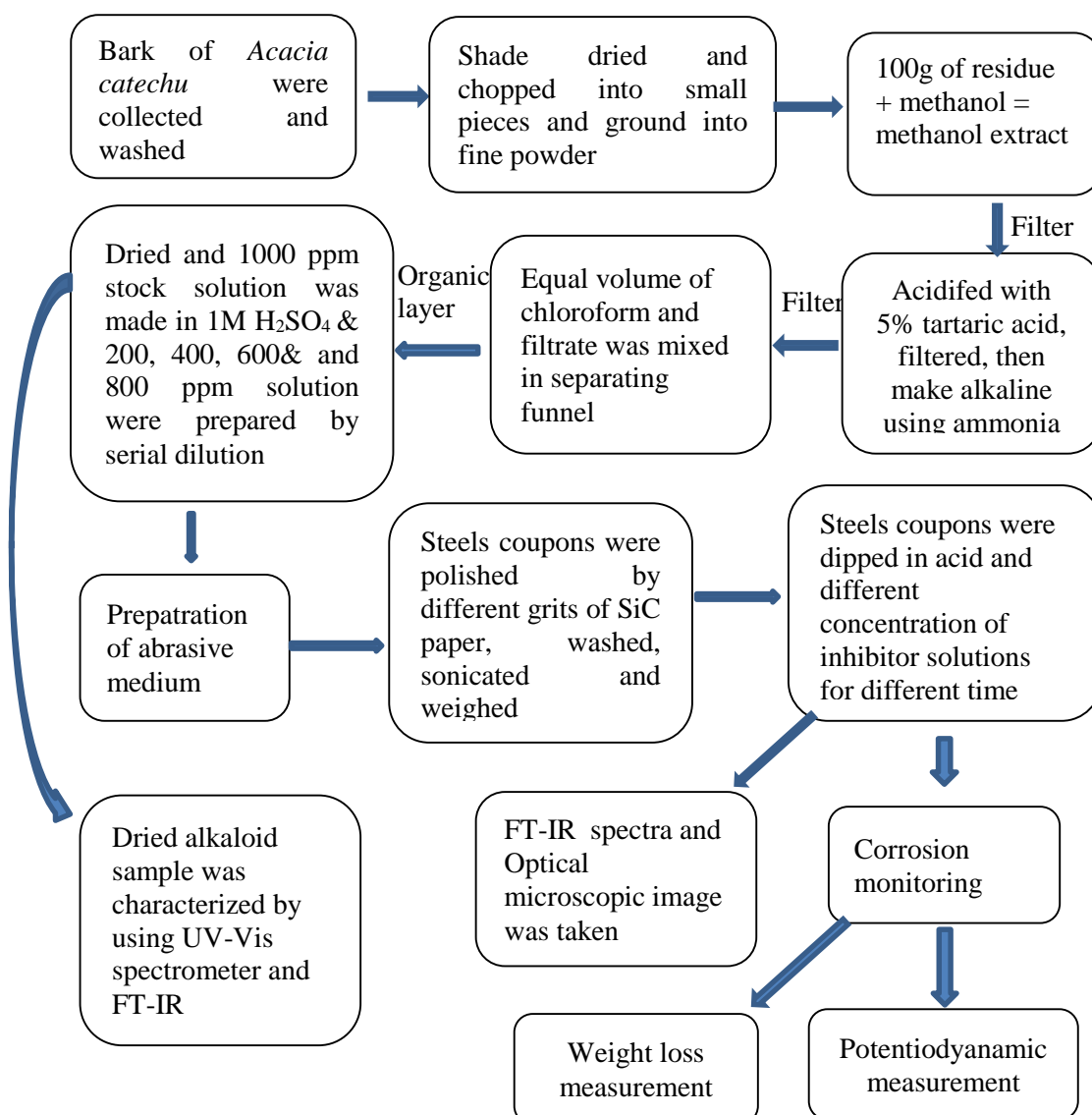


Figure 5: Schematic Chart of Methodology

## CHAPTER 4

### RESULTS AND DISCUSSION

The weight-loss method, open circuit potential, and potentiodynamic polarization were used to investigate the alkaloid's corrosion inhibitory action on MS. Qualitative chemical tests, UV spectroscopic, and FTIR spectroscopic measures were used to characterize alkaloids. An optical microscope was also used to take the image of immersed MS.

#### 4.1 Test of Alkaloids

A qualitative test for the confirmation of alkaloids extracted from *Acacia catechu* was performed. The test of alkaloids in different reagents was tabulated as in table 1.

Table 1: Phytochemical screening of the extract solution

S.N.	Experiment	Result	Inference
1.	Mayer's Test	The appearance of the orange precipitate.	+ve
2.	Dragendroff 's Test	The appearance of orange-red color.	+ve
3.	Wagner's Test	The appearance of a reddish-brown precipitate.	+ve

#### 4.2 UV Spectroscopic Measurements

The UV measurement is used to determine whether an organic compound is unsaturated or contains a lone pair of electrons. In Amrit Campus, Kathmandu, the UV spectra of alkaloids were recorded using a Labtronics LT-2802 double beam ultraviolet-visible (UV-Vis) spectrometer.

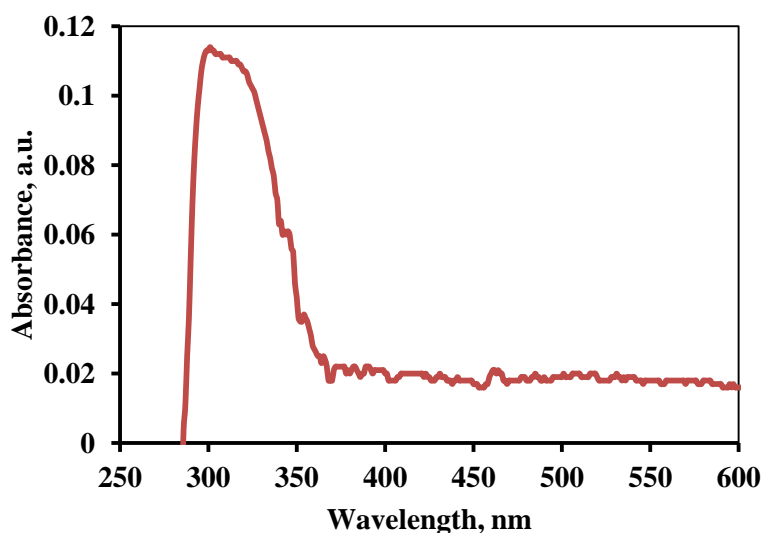


Figure 6: UV-Vis spectrum of an alkaloid of *Acacia catechu*

In the spectra in figure 6, the sharp peak at 305 nm to 348 nm indicates the presence of lone pair of electrons and the unsaturation in the compound. The sharp peak at 311 nm is due to the  $n-\pi^*$  transition of the alkaloids (Silverstein and Webster, 2006).

### 4.3 FT-IR Analysis

The FTIR spectroscopic study of organic compounds can be used to determine the kind of bonding,  $\pi$ -bond conjugate system, aromatic and aliphatic structures, and, most importantly, the functional group present. PerkinElmer Spectrum IR Version 10.6.2 FTIR spectrometer was used to record the FTIR spectrum of *Acacia catechu* alkaloid extract, as shown in figure 7. The FTIR spectrum reveals the chemical structure and confirms the presence of organic molecules as well as various functional groups in the sample. The stretching frequency in the FTIR spectrum can be used to identify the carbon-heteroatom bond.

The FTIR spectra of the ACBA extract with typical functional groups are shown in Figure 6. O-H stretching of alcohol, phenol, carbohydrate, and N-H stretching of amine are responsible for the  $3360\text{ cm}^{-1}$  to  $3209\text{ cm}^{-1}$  bandwidth. A band at  $2912\text{ cm}^{-1}$  depicts alkane C-H stretching, whereas a band at  $1650\text{ cm}^{-1}$  symbolizes C=C stretching, C=N stretching imine or oxime, amide, or  $\delta$ -lactum C=O stretching, and amine N-H bending.

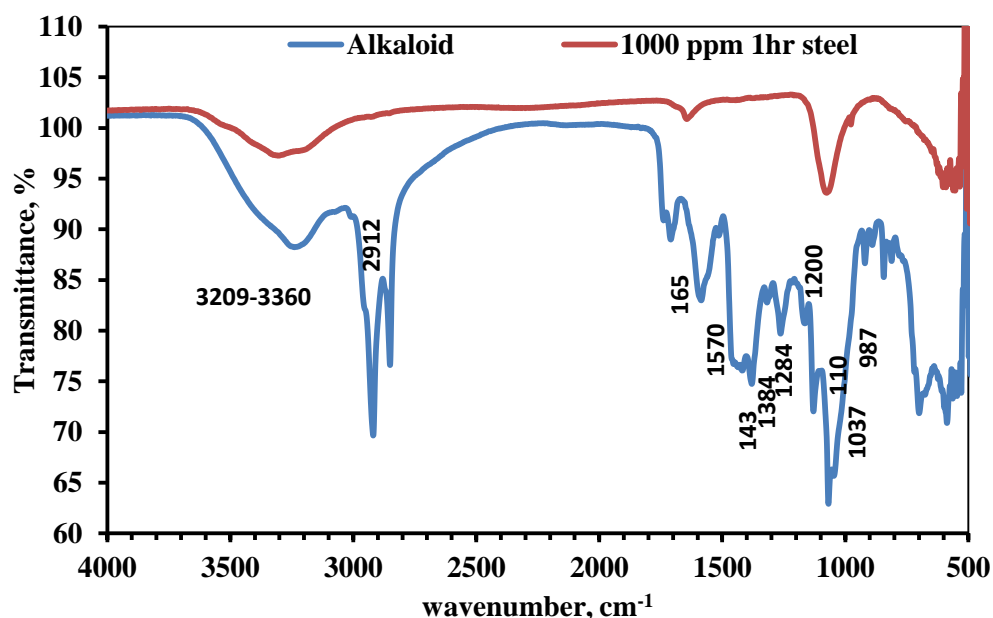


Figure 7: FT-IR spectrum of alkaloid and steel immersed in 1000 ppm inhibitor for 1 hr

Aromatic C=C bending and N-H bending of amine are coupled with a sharp band at  $1570\text{ cm}^{-1}$ . Similarly, the absorption band at  $1435\text{ cm}^{-1}$  is due to carboxylic acid O-H

bending, and a strong peak at  $1384\text{ cm}^{-1}$  is owing to alcohol, phenol, and gem dimethyl or aldehyde C-H bending. A band at  $1284\text{ cm}^{-1}$  is attributed to aromatic amine C-N stretching, which is corroborated by a strong peak at  $1037\text{ cm}^{-1}$ . The absorption band at  $1200\text{ cm}^{-1}$  is caused by C-O stretching of aromatic ether,  $3^\circ$  alcohol, ester, and C-N stretching of amine, whereas the band at  $1103\text{ cm}^{-1}$  is caused by C-O stretching of  $2^\circ$  alcohols, ether, and C-N stretching of amine. Because of the alkene's C=C bending, there is another band at  $987\text{ cm}^{-1}$  (Karki, et al., 2020). It's very interesting that the peaks around  $2900\text{ cm}^{-1}$  are absent in the spectra of the alkaloids adsorbed on MS surface. This implies that the polar nitrogen containing alkaloids only able to get adsorbed in the MS surface rather than alkaloids with bulky aromatic groups.

#### **4.4 Optical microscopy image**

An OM image of polished MS, acid dipped and 1000 ppm inhibitor dipped MS was taken by the optical microscopy instrument (Model: RXLT-4 Radical Scientific, India) at the Central Department of Chemistry, Tribhuvan University, Nepal. In the presence of inhibitor and acid, the production of corrosion products (small pits and rusts) was detected, but no corrosion products were visible in polished (undipped) MS coupons. The large pits and more rusts were seen due to the reaction between the acid molecules and the MS surface in acid dipped MS but in the case of MS dipped in 1000 ppm inhibitor solution, there are generally small pits and little rusts. This means the inhibitor molecules block a large number of acid molecules to react with the MS surface. The greenish-brown patches over the MS surface dipped in 1000 ppm inhibitor solution were observed as in the figure below which indicates the adsorption of inhibitor molecules on the MS surface. But in the case of undipped MS, there are no acid molecules to react so it has no pits and rusts. The images were taken at a magnification scale of 4x, 10x, and 40x which are shown in figure 8 below.

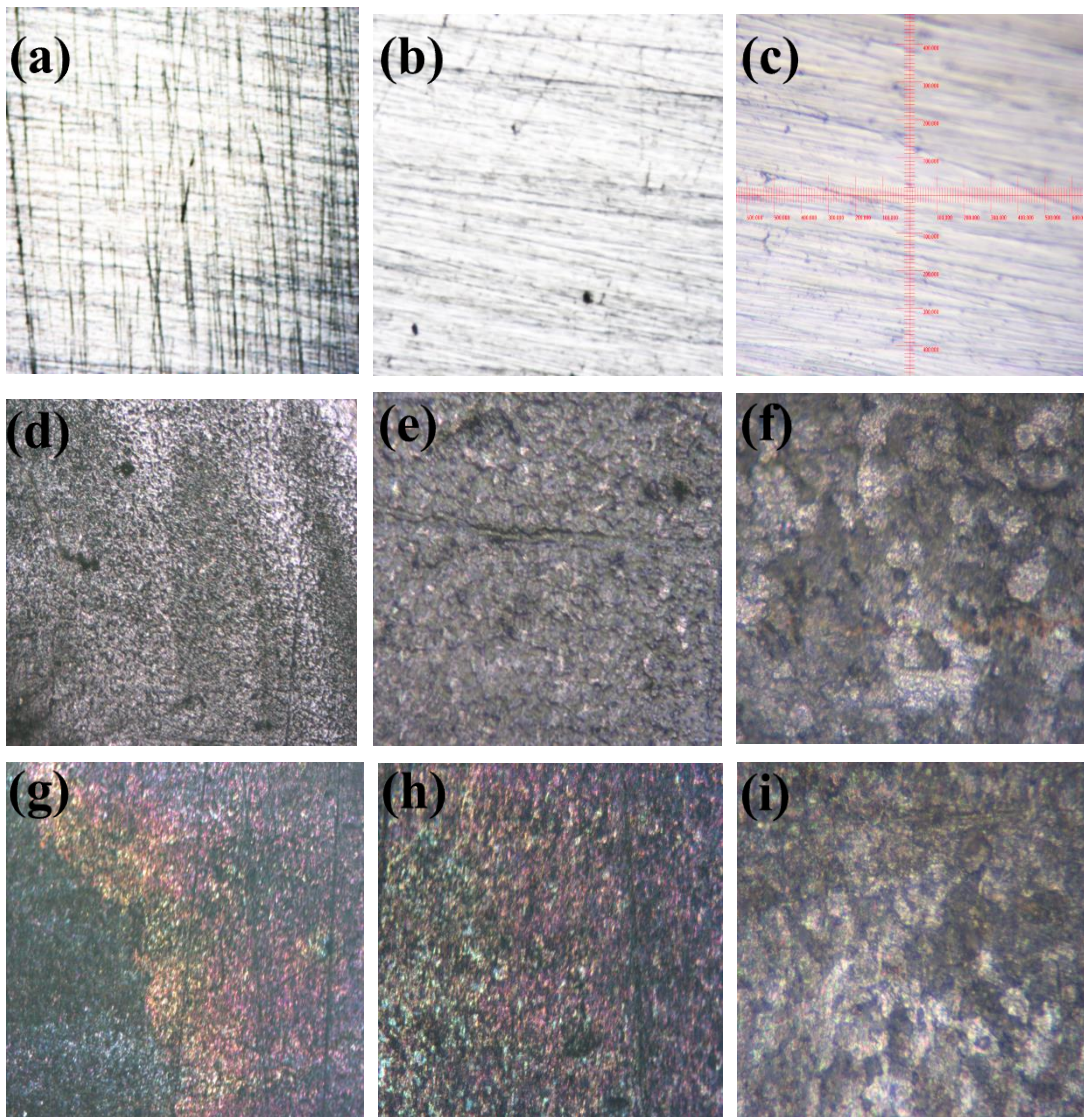


Figure 8: OM image of polished MS: (a) at 4x (b) at 10x (c) at 40x OM image of MS in acid: (d) at 4x (e) at 10x (f) at 40x OM image of MS in 1000 ppm inhibitor: (g) at 4x (h) at 10x (i) at 40x

## 4.5 Weight Loss Measurements

### 4.5.1 Variation of weight loss with immersion time

Figure 9 shows the results of the weight loss experiment for MS immersed in 1 M  $\text{H}_2\text{SO}_4$  with and without inhibitor. The inclusion of an alkaloid inhibitor reduces metal weight loss in the acidic inhibitor medium when compared to 1M  $\text{H}_2\text{SO}_4$  solution, according to the weight loss measurement. Experiments were carried out in 1 M  $\text{H}_2\text{SO}_4$  in the presence and absence of inhibitor at different periods, namely 0.5, 1, 3, 6, and 24 hours at 18 °C.

It shows that when the duration is increased, the weight loss of metal increases in

both, but the ratio of weight loss decreases in inhibitor when compared to 1M H<sub>2</sub>SO<sub>4</sub>. Because the inhibitors are adsorbed on the MS surface, an adsorptive layer forms. This adsorptive layer served as an acid barrier. The weight loss of the MS is almost constant from 6 h onwards. It may be due to the formation of passive layer of inhibitor which completely block the reaction between the acid molecules and the MS surface results in the stoppage of further weight loss even in increasing the immersion time.

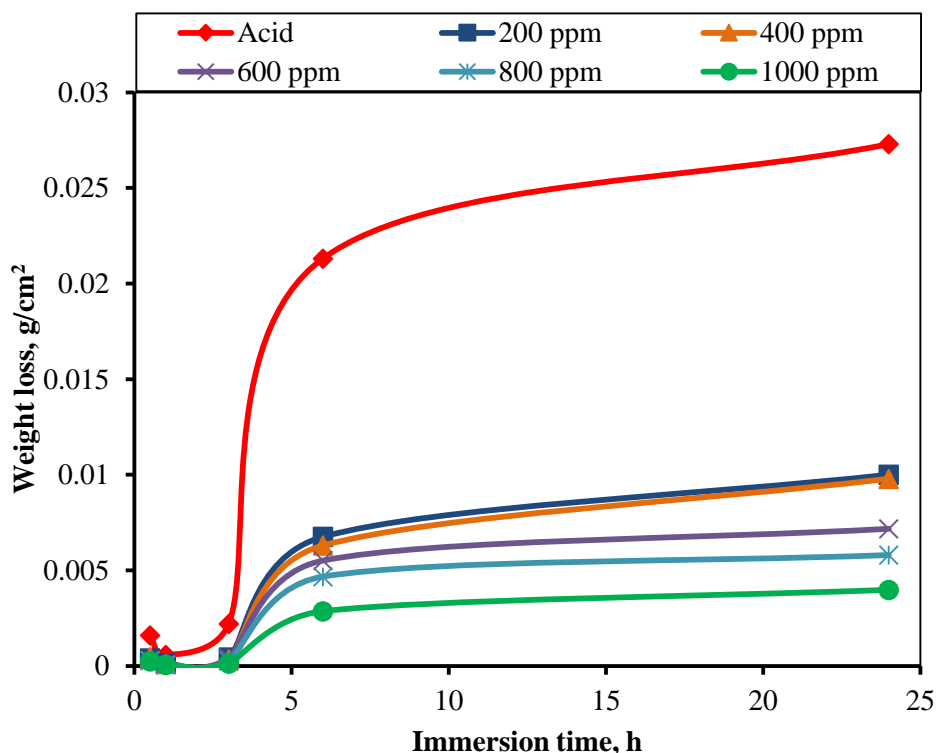


Figure 9: Variation of weight loss with immersion time for the corrosion of mild steel in the solution of 1M H<sub>2</sub>SO<sub>4</sub> and solution of different inhibitor concentrations at room temperature.

Table 2 shows the weight loss of MS coupons in grams per unit area. In compared to inhibitor solutions, the weight loss of MS in acid is quite substantial. Although there is weight loss in the presence of the inhibitor solution, it is much lower than in the absence of the inhibitor solution. This reduction in weight loss is related to inhibitor inhibition. The weight loss of MS for a half-hour immersion period is quite low, but the associated inhibitory efficiency is not particularly great. This is because inhibitor molecules do not completely cover the MS surface at first. The weight loss rises in all cases as the immersion duration increases, but the associated inhibition efficiency improves, demonstrating the inhibitor molecule's inhibitory action.

Table 2: Variation of weight loss (g/cm<sup>2</sup>) with different immersion time at different concentrations of inhibitors.

Time(hr)	Weight loss (g/cm <sup>2</sup> )					
	Acid	200 ppm	400 ppm	600 ppm	800 ppm	1000
0.5	0.00160	0.00039	0.00046	0.00027	0.00027	0.00025
1	0.00058	0.00014	0.00012	0.00007	0.00007	0.00006
3	0.00220	0.00044	0.00035	0.00027	0.00027	0.00013
6	0.02131	0.00676	0.00630	0.00467	0.00467	0.00287
24	0.02729	0.01001	0.00979	0.00580	0.00580	0.00398

The inhibition efficiency of the inhibitor molecules of different concentrations in 1 M H<sub>2</sub>SO<sub>4</sub> for MS samples is shown in Figure 10. The inhibition efficiency of the 1000 ppm inhibitor solution is the highest. The maximum inhibition efficiency is found to be 85.40 % of 1000 ppm solution at 24 h immersion time.

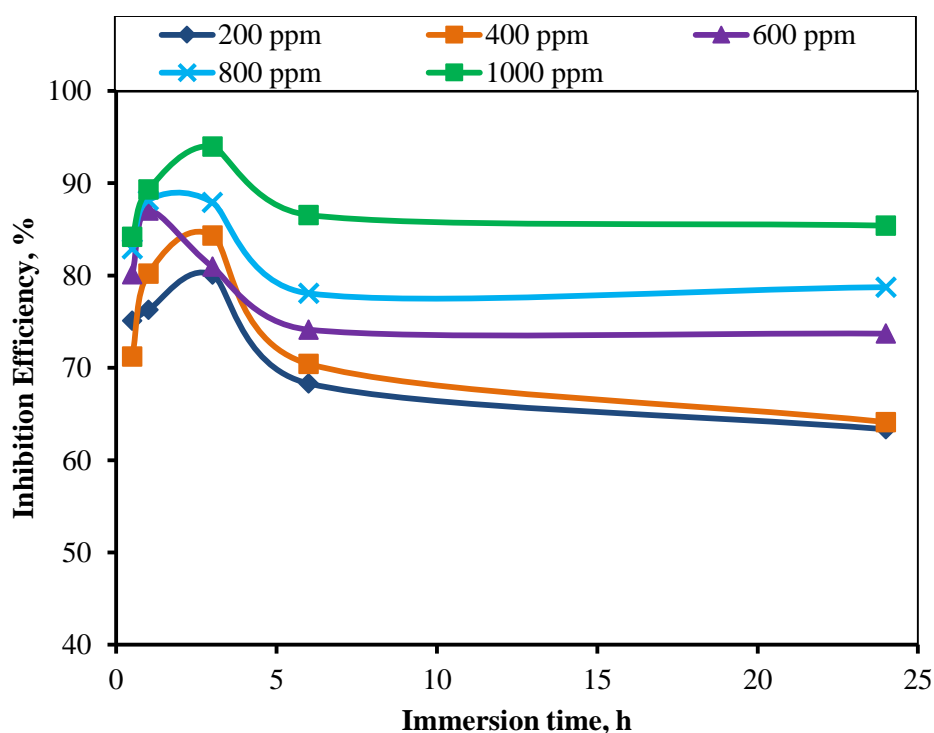


Figure 10: Variation of inhibition efficiency of different inhibitor solutions in 1M H<sub>2</sub>SO<sub>4</sub> solution vs time for the corrosion of mild steel at various times.



#### 4.5.2 Weight loss of MS in different concentrations of alkaloid at different time

When MS coupons are dipped in the acid solution, the acid interacts with the MS surface, causing corrosion products to develop. The weight of MS has reduced as a result of the production of the corrosion product. The weight of MS coupons decreases as the nature of the MS surface, temperature, and solution concentration change. MS has a significant weight loss in the absence of an inhibitor.

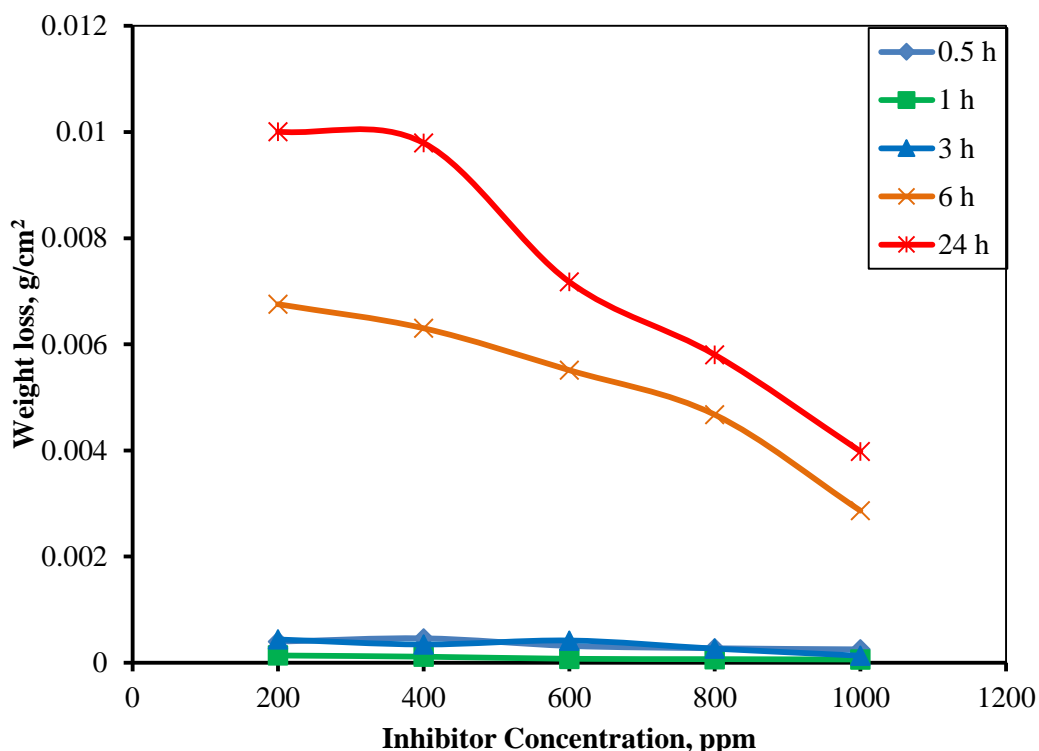


Figure 11: Variation of weight loss versus concentration of extract on mild steel in 1 M H<sub>2</sub>SO<sub>4</sub> solution at various times.

As demonstrated in Figure 11, the loss in weight of MS diminishes progressively as the concentration of inhibitor increases up to 6 hr. It might be due to inhibitor molecule adsorption on the metal surface. At 1 hour, all the concentrations caused the least weight loss and at 1000 ppm weight loss increased which is not possible, so this may be due to the handling error. In 24 hr the weight loss is more significant than 1 hr, 3 hr, and 6 hr, it can be due to the desorption of inhibitor molecule at a long time interval (Karki, et al., 2020).

#### 4.5.3 Inhibition efficiency by different concentrations of alkaloid

The inhibitor concentration has a significant impact on the inhibitor's ability to inhibit. The inhibitory efficacy of inhibitor solution at all concentrations is greater

than 50% throughout any immersion period in this experiment except at 200 ppm at 6 hrs. This demonstrates that there is enough inhibitor present to completely cover the MS surface, leading to substantially higher inhibition. An increase in the surface coverage of the MS by the inhibitor molecule is indicated by the increasing order in which inhibition occurs with concentration. For maximal inhibition, a concentration of 1000 ppm is the ideal inhibitor solution. In 6 hrs and 24 hrs of exposure, its inhibitory effectiveness peaked because at 1000 ppm there is enough inhibitor molecule to get adsorbed in the surface of MS resulting in the minimum weight loss which alternately increases the efficiency. The inhibitory effects of the inhibitor at various concentrations are presented in the table below.

*Table 3: Inhibition efficiency (%) of different concentrations of inhibitor at different immersion time*

Time (hr)	Inhibition efficiency (%)				
	200 ppm	400 ppm	600 ppm	800 ppm	1000 ppm
0.5	75.11	71.22	80.14	82.91	84.18
1	76.28	80.19	87.03	88.15	89.30
3	80.08	84.34	80.96	87.92	93.96
6	68.30	70.43	74.13	78.07	86.55
24	63.34	64.12	73.71	78.74	85.41

Usually, there is an increase in inhibition efficiency from low to the high concentration of inhibitor at any time of immersion and maximum at 1000 ppm concentration. But there is a decrease in efficiency in 1 hr for 1000 ppm which may be due to the handling error.

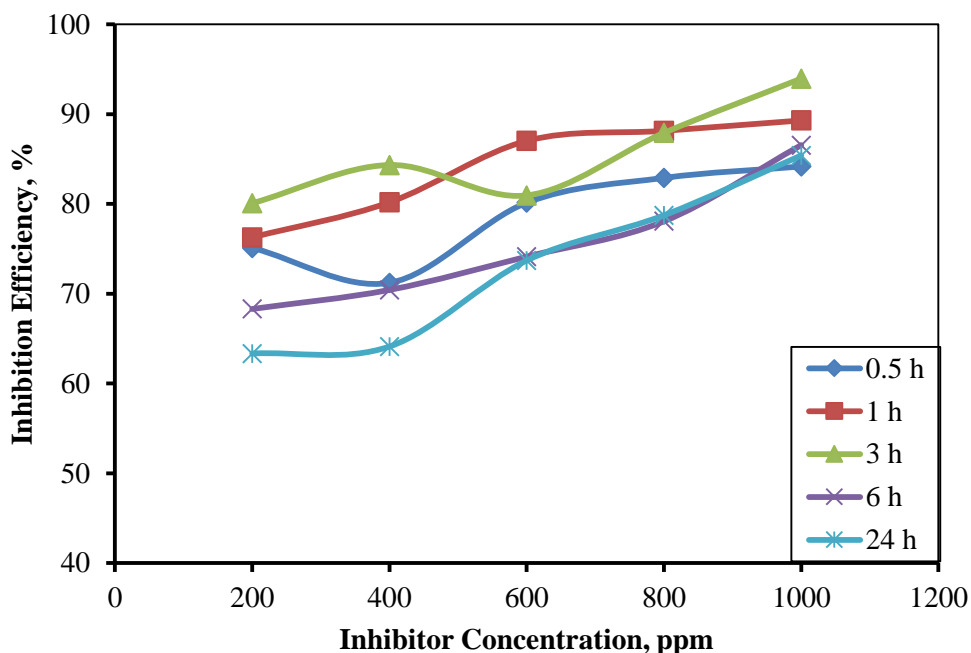


Figure 12: Inhibition efficiency at different concentrations of inhibitor on mild steel in 1 M  $H_2SO_4$  solution at various times

#### 4.5.4 Variation of weight loss with temperature

The influence of temperature on the inhibition process was investigated using three different doses of inhibitor solution (200, 600, and 1000 ppm). The weight loss in these three distinct inhibitor solutions at different temperatures was calculated using the acid solution as a reference. The MS coupons were submerged in these solutions for one hour at various temperatures (28, 38, 48, and 58 °C) for this measurement. Table 3 summarizes the observed data.

Table 4: Weight loss ( $g/cm^2$ ) of MS immersed in different concentrations of inhibitor at different temperatures

Temperature(°C)	Weight loss ( $g/cm^2$ )			
	Acid	200 ppm	600 ppm	1000 ppm
28	0.00437	0.00257	0.00112	0.00045
38	0.01085	0.00610	0.00305	0.00143
48	0.01829	0.01573	0.00840	0.00285
58	0.02531	0.02484	0.02322	0.01822

MS weight loss is greatest in acid solution and lowest in 1000 ppm inhibitor solution. MS weight loss in inhibitor solutions increased with increasing temperature. This increase in weight loss might be attributed to two factors: desorption of the inhibitor

molecules from the MS surface or structural distortion of the inhibitor molecules (Andoor, et al., 2021). As weight reduction progresses, the inhibitor's inhibitory effectiveness decreases.

The effect of higher temperatures is to speed up a chemical reaction and reduce oxygen solubility, which allows the cathodic reaction to occur. In addition, the viscosity of water decreases with temperature increases; this leads to increased diffusion, which will allow increased transport of reactants (dissolved oxygen or other electrons acceptors) and product ( $\text{Fe}^{+2}$  species) on the metal surface and increased weight loss which in turn decrease the inhibition efficiency (Khaleel, et al., 2018).

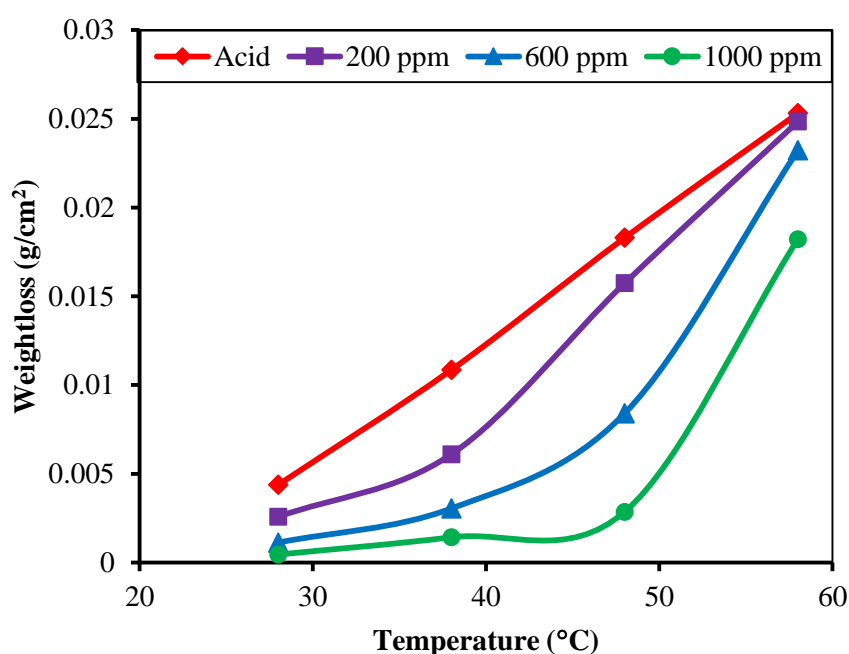


Figure 13: Variation of weight loss of mild steel coupons in 1 M  $\text{H}_2\text{SO}_4$  and 200, 600, and 1000 ppm inhibitor at different temperatures.

As shown in figure 13, the loss of weight is usually small at low temperature and increases on increasing the temperature which can be predicted that the inhibitor molecule becomes unstable at high temperature resulting in decreases in its effectiveness.

#### 4.5.5 Effect of Temperature on Inhibition Efficiency

The temperature harms the IE%. The increase in temperature leads to an increase in the dynamic energy for the inhibitor molecules. This raises the rate of their collision with each other. This in turn impedes and slows the formation of the protective film

of inhibitors on the metal surface. Thus increase in temperature affects the strength of the adsorption molecules on the metal surface (Khaleel, et al., 2018). The impact of temperature on corrosion inhibition with and without inhibitors was investigated using varying temperatures and a constant immersion period of 1 hour. Table 5 summarizes the inhibition efficiency against temperature.

*Table 5: Inhibition efficiency (%) of the inhibitor of different concentrations on MS at different temperatures*

Temperature (°C)	Inhibition efficiency (%)		
	200 ppm	600 ppm	1000 ppm
28	41.22	74.31	89.73
38	43.82	71.92	86.88
48	13.99	54.07	84.39
58	1.85	8.26	28.02

It is obvious from the table that the inhibitory efficiency of 200 ppm inhibitor solution is essentially minimal at all temperatures, with an additional intriguing feature that there is no effect of temperature up to 48 °C for 1000 ppm inhibitor solution. Up to 38 °C, there is satisfactory inhibition efficiency in 600 ppm inhibitor solution. There is a very low efficiency of 1000 ppm at 58 °C which is 28.02 %. After these results, it can be concluded that the structural deformation of molecules may occur more than that of the desorption of molecules from the MS surface. This deformation leads to the decrease in inhibition efficiency of inhibitors for MS in an acidic medium. Results show less thermal stability of inhibitors at high temperatures.

Figure 14 depicts the temperature-dependent fluctuation in inhibitory efficiency. The figure clearly shows that the 200 ppm inhibitor solution is almost ineffective at all temperatures. Up to 48 °C, the 1000 ppm inhibitor solution inhibited well and at 28 °C, the inhibition efficacy of a 1000 ppm inhibitor solution was maximum. After 48 °C the inhibition efficacy of 1000 ppm is decreasing further increasing the temperature by forming the hump shape as shown in the figure.

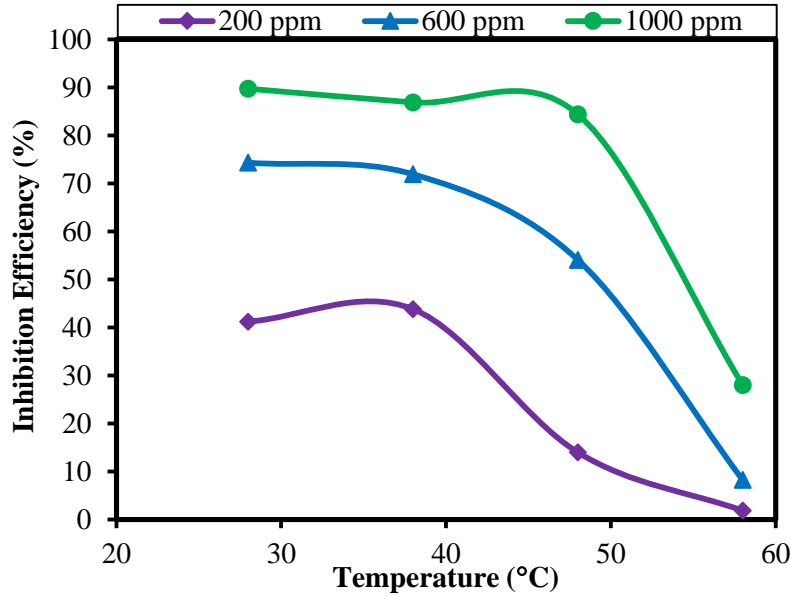


Figure 14: Variation of inhibition efficiency with temperature on the mild steel in presence of 200, 600, and 1000 ppm inhibitor in 1 M H<sub>2</sub>SO<sub>4</sub> solution.

#### 4.6 Adsorption Isotherm

When solid things are submerged in solutions, molecules from the solution get adsorbed on the solid surface. Similarly, MS coupons are submerged in acid as well as inhibitor solution in this case. When MS is submerged simply in acid solution, the acid molecules are absorbed and a violent reaction ensues, causing the MS coupon to deteriorate. Similarly, in the presence of an acid-inhibitor solution mixture, inhibitor molecules are first adsorbed on the MS surface, resulting in a reduction in MS degradation. The adsorption isotherm should be known for a thorough comprehension of this adsorption process. Adsorption isotherms should be checked for a better understanding of the adsorption isotherm and the kind of adsorption between the MS surface and the inhibitor molecule.

The adsorption isotherm provides fundamental information about the interaction between the inhibitor and the MS surface. Water molecules are initially adsorbed on the MS surface in an aqueous solution. After that, inhibitor molecules replace the adsorbed water molecules. As a result, aqueous solution adsorption of inhibitor compounds is a quasi-substitution process. To identify the adsorption isotherm, Langmuir adsorption isotherm was determined. Langmuir adsorption isotherm equation can be applied to find whether the adsorption process is monolayer or

$$\text{multilayer as, } \frac{C_{inh}}{\theta} = \frac{1}{K_{ads}} + C_{inh} \quad \dots (6)$$

This equation is like the equation of a straight line as  $y = mx + c$ . The linear relation between the fraction of covered surface ( $\theta$ ) value and  $C_{inh}$  should be known to find the adsorption isotherm. The linear relation between the fraction of covered surface ( $\theta$ ) and molar concentration ( $C_{inh}$ ) should be known to find the adsorption isotherm. If the slope of the curve obtained by plotting  $C/\theta$  vs  $C_{inh}$  in the above equation is unity then it indicates the monolayer adsorption. As in the equation if one uses the molar concentration of the inhibitor then the value of adsorption constant  $K_{ads}$  can be calculated from the intercept of a straight line.

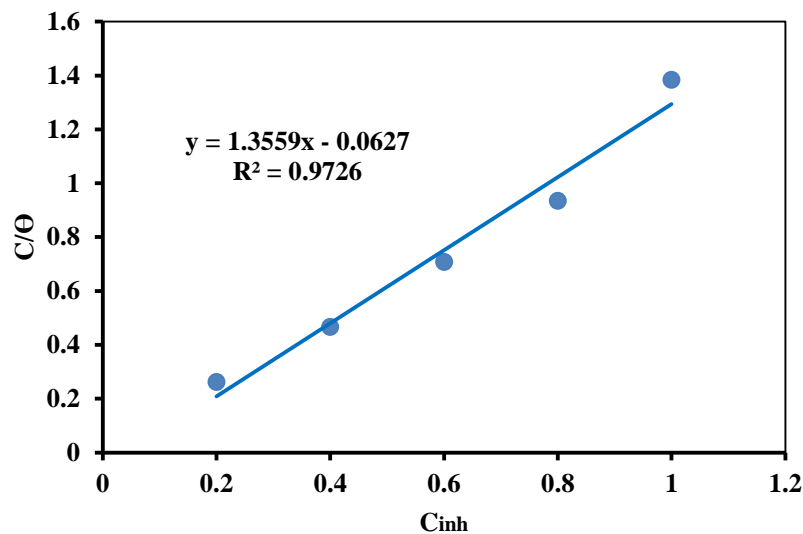


Figure 15: Langmuir adsorption isotherm plot for MS in 1 M  $H_2SO_4$  with different concentrations of inhibitor.

As in figure 15, the value of regression coefficient ( $R^2$ ) and the slope are not near to unity which means the inhibitors molecules are not adsorbed on the MS surface according to Langmuir adsorption isotherm. This suggests that adsorption can be mono-layer or multilayer, but that the entire monolayer did not occur before the creation of the multilayer. The slope and  $R^2$  values diverged significantly from unity, implying that the adsorption mechanism in this corrosion inhibition process cannot be described by this Langmuir isotherm (Andoor, et al., 2021; Ituen, et al., 2017).

#### 4.7 Activation Energy

The activation energy of a process in an electrochemical cell in the presence and absence of an inhibitor may be described by rearranging the Arrhenius equation. The activation energy of the process is proportional to the corrosion rate as follows:

$$\log(CR) = \log A - \frac{E_a}{2.303RT} \quad \dots (7)$$

Where A is the Arrhenius pre-exponential constant, T is the absolute temperature. Equation (7) shows that the activation energy of the reaction is equal to the slope of the Arrhenius plot i.e. a plot obtained between logarithms of corrosion rate with  $\frac{1}{2.303RT}$  along axes.

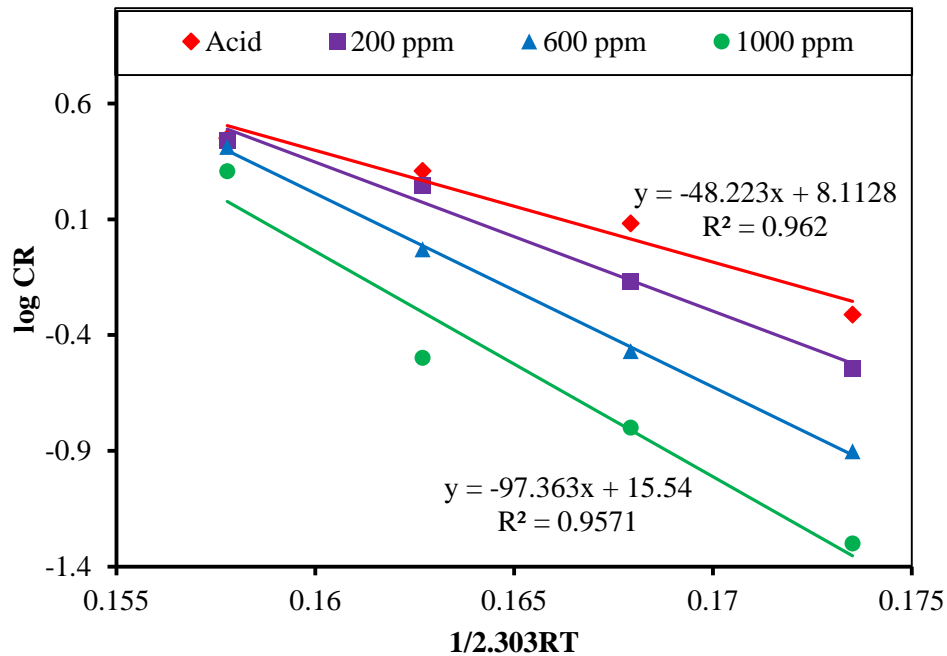


Figure 16: Arrhenius plot for MS in 1M H<sub>2</sub>SO<sub>4</sub> with and without inhibitor

Here, the activation energy for the reaction between an acid and mild steel is 48.22 KJ/mol. When the inhibitor is added then the energy of activation is increased due to the blockage of acid molecules to the MS surface by the inhibitor molecules. The energy of activation is 64.38 KJ/mol, 83.60 KJ/mol, and 97.36 KJ/mol for 200 ppm, 600 ppm, and 1000 ppm inhibitor solution respectively (Figure 16).

This rise in activation energy indicates that when inhibitor molecules are added, the reaction rate between acid and MS is suppressed, leading to a drop in corrosion rate. These computed values fall somewhere between physical (less than or equal to 20 kJ/mol) and chemical (more than 80 kJ/mol). Adsorption of alkaloids on MS surface in 1M H<sub>2</sub>SO<sub>4</sub> solution, therefore, comprises a mixed kind of adsorption with chemisorption dominance (Karki, et al., 2021).



#### 4.7.1 Enthalpy and Entropy measurement

Enthalpy and entropy of the system can be calculated by using the transition state equation, an alternative form of the Arrhenius equation,

$$\log\left(\frac{CR}{T}\right) = \log\left(\frac{R}{hN_A}\right) + \frac{\Delta S^\circ}{2.303R} - \frac{\Delta H^\circ}{2.303RT} \quad \dots (8)$$

Where, h is plank's constant,  $6.6261 \times 10^{-34}$  Js, and  $N_A$  is the Avogadro's number,  $6.0225 \times 10^{23} \text{ mol}^{-1}$ .

Enthalpy of activation ( $\Delta H^\circ$ ) is obtained as the slope of a straight line by plotting the  $\log\left(\frac{CR}{T}\right)$  vs  $\frac{1}{2.303RT}$  and entropy of activation ( $\Delta S^\circ$ ) from its intercept (Karki, et al., 2021).

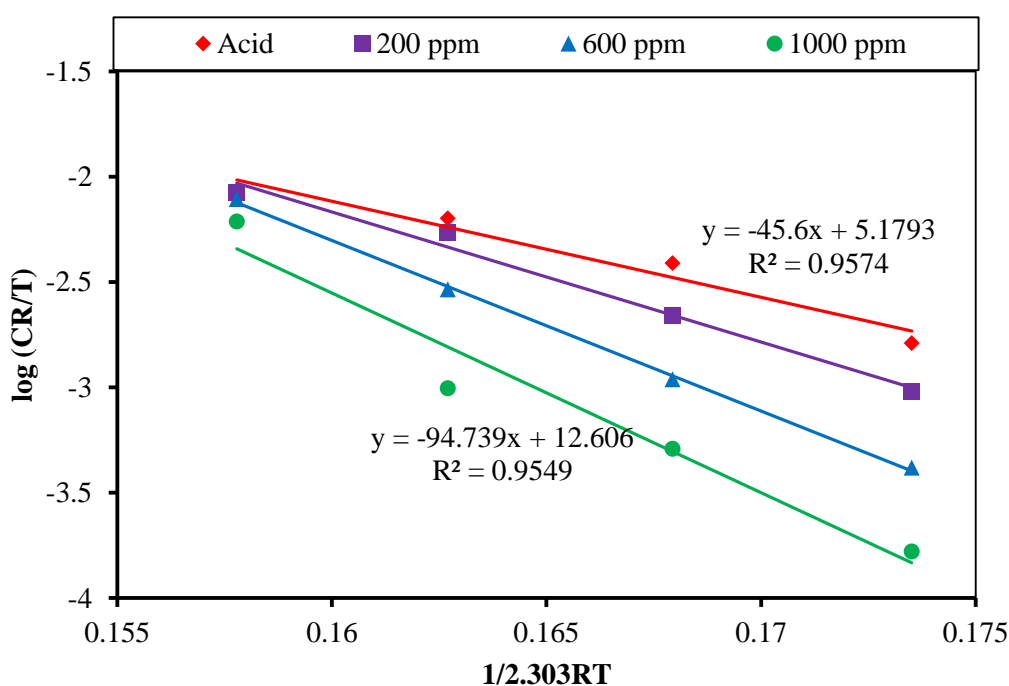


Figure 17: Transition state plot for MS in 1M H<sub>2</sub>SO<sub>4</sub> with and without inhibitor.

From the above figure 17, the enthalpy of activation was found to be 45.60 KJ/mol in absence of an inhibitor and increases to 61.76 KJ/mol, 80.97 KJ/mol, and 94.74 KJ/mol for 200 ppm, 600 ppm, and 1000 ppm respectively. The positive value of  $\Delta H^\circ$  for inhibitor adsorption on the MS surface suggests that the adsorption is an endothermic process. The progressive increase in enthalpy value implies a decrease in corrosion rate regulated by activation kinetic factors. The participation of a gaseous reaction, i.e. cathodic hydrogen evolution process, leads to a reduction in total reaction volume when  $E_a$  is greater than  $\Delta H^\circ$ . The values of  $E_a$  and  $\Delta H^\circ$  also show that alkaloid adsorption occurs through both physical and chemical interactions (Karki, et al., 2021; Ituen, et al., 2017).

The degree of randomness of the molecules is calculated from the intercept of the transition state plot. The calculated value of entropies is -98.42, -49.86, 6.42, and 43.80 J<sup>-1</sup>mol<sup>-1</sup>K for acid, 200 ppm, 600 ppm, and 1000 ppm solutions respectively. This increase in the entropy reveals that there is quasi-substitution process where the water molecule adsorbed on MS surface is replaced by inhibitor molecules as well as due to decrease in the evolution of hydrogen, the hydrogen ion roams in the electrolyte medium. The addition of three different doses of inhibitors boosted the system's activation energy. An increase in activation energy decreases the reaction rate, which suppresses the corrosion rate. With the addition of an inhibitor, the rise in  $E_a$  demonstrates the high adsorption of inhibitor molecules on the metal surface, with total or almost complete coverage, such that acid molecules have little or no possibility of reacting with the metal. The calculated values of  $E_a$ ,  $\Delta H^\circ$ , and  $\Delta S^\circ$  for acid without and with inhibitor are tabulated in Table 6.

*Table 6: Activation parameters of the MS dissolution in 1 M H<sub>2</sub>SO<sub>4</sub> without and with inhibitor.*

Electrolyte	$E_a$ (kJ/mol)	$\Delta H^\circ$ (kJ/mol)	$\Delta S^\circ$ (J/mol/K)
1M H <sub>2</sub> SO <sub>4</sub>	48.22	45.60	-98.42
1M H <sub>2</sub> SO <sub>4</sub> + 200 ppm Inhibitor	64.38	61.76	-49.86
1M H <sub>2</sub> SO <sub>4</sub> + 600 ppm Inhibitor	83.60	80.97	6.42
1M H <sub>2</sub> SO <sub>4</sub> + 1000 ppm Inhibitor	97.36	94.74	43.80

## 4.8 Electrochemical Methods

### 4.8.1 Open circuit potential (OCP) measurement

By observing variations in corrosion potential over time, the fluctuation of mild steel's open circuit potential (OCP) in 1 M H<sub>2</sub>SO<sub>4</sub> was investigated. The OCP modifications of MS were exposed to acid solutions and inhibitors at various concentrations (200, 400, 600, 800, and 1000 ppm) for 30 minutes at 18 °C. The change in OCP over time was measured using a three-electrode method. Figure 18 shows the results of the OCP measurement in the presence of inhibitor solutions at various concentrations. It demonstrates that, in the presence of an inhibitor, there is a minor change in potential toward an increase in OCP toward a positive potential, but this shift is less than 50 mV. This suggests that it may have mixed inhibitory effects. The creation of a protective layer on the MS surface by inhibitor molecules in acid solution, as indicated by the positive shifting of potential from OCP, inhibits the interaction of

hostile ions with the MS surface.

Figure 18 shows that initially, the potential shifted to more positive, but the shift in the value of OCP is less than 50 mV indicating plant extract act as a mixed corrosion inhibitor. The shifting of potential from OCP to more positive indicates that the MS surface is positively charged which when interacts with alkaloids forms a protective layer. This protective layer by alkaloid molecules in acid solution on the MS surface, (i.e. passivation) limits the interaction of aggressive ions with the MS surface (Ijuo et al., 2016; Karki et al., 2021).

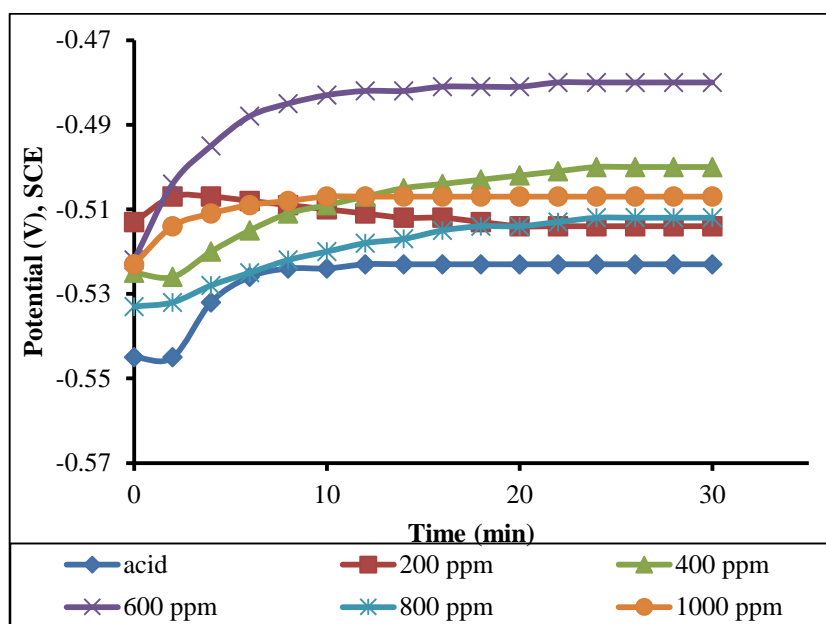


Figure 18: Variation of OCP with the time of immersion of mild steel in different concentrations of inhibitor in 1M H<sub>2</sub>SO<sub>4</sub> measured at the time of immersion.

But in figure 19, there is a slight increase in OCP towards negative potential because there is no inhibitor molecule. In the case of the solution having different concentrations of inhibitor, there is a slight increase in OCP towards positive potential firstly and remains constant after a certain time.

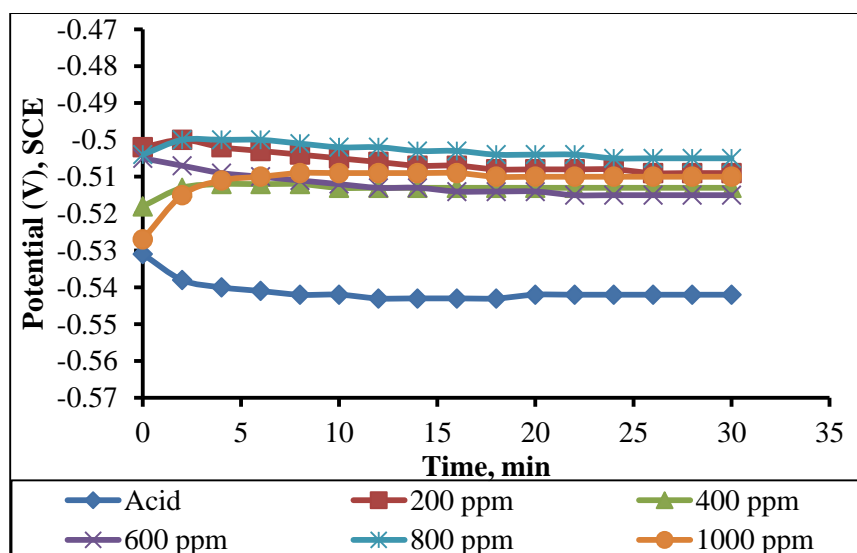


Figure 19: Variation of OCP with the time of immersion of mild steel in different concentrations of inhibitor in 1M  $H_2SO_4$  measured after 3 h immersion in solutions.

#### 4.8.2 Polarisation measurement of As - immersed MS

Polarization of mild steel samples in acid and various inhibitor concentrations (200, 400, 600, 800, and 1000 ppm) was accomplished by applying  $\pm 350$  mV in both anodic and cathodic directions using a potentiostat. The Evans diagram and Tafel extrapolation show that the reduction in current density with the addition of inhibitor signifies that the MS surface is covered with inhibitor molecules, resulting in a tiny active site for the process.

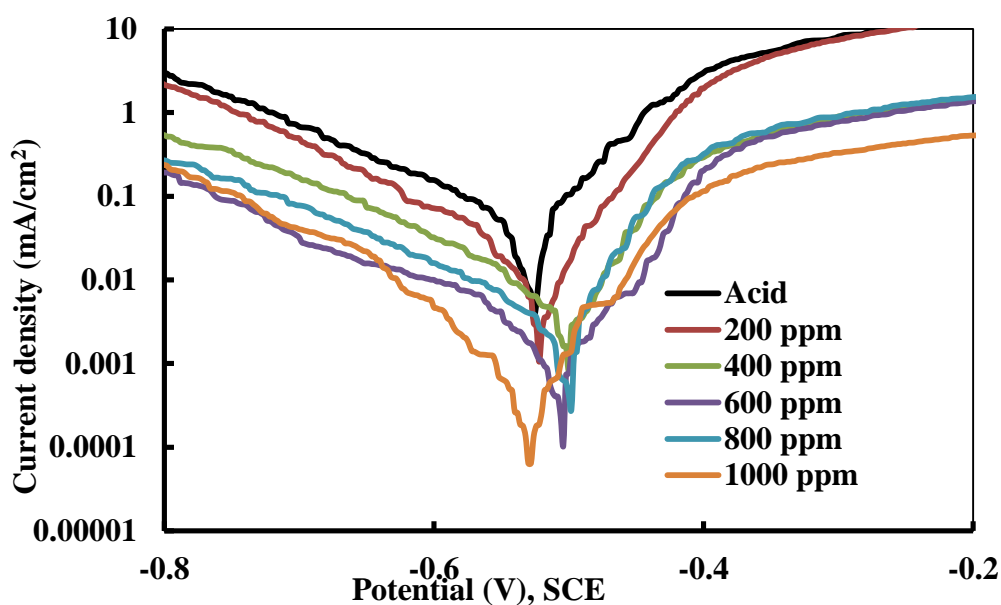


Figure 20: Potentiodynamic polarization curves for mild steel in 1M  $H_2SO_4$  containing different concentrations of inhibitor as-immersed condition.

This polarization measurement of MS was carried out at a laboratory temperature of 18 °C and the obtained results were tabulated in table 7. The result of the decrease in the corrosion current in presence of an inhibitor indicates the blockage of reacting sites by inhibitor molecules.

Table 7: Anodic and cathodic slope and inhibition efficiency for as-immersed sample.

Medium	OCP (V)	Anodic Slope (V/decade)	Cathodic Slope (V/decade)	I <sub>corr</sub> (mA/cm <sup>2</sup> )	Inhibition Efficiency (%)
Acid	-0.526	14.7	6.5	0.0486	-
200 ppm	-0.519	13.4	4.8	0.0127	73.87
400 ppm	-0.504	14.2	5.1	0.0072	85.19
600 ppm	-0.507	11.8	4.8	0.0023	95.27
800 ppm	-0.497	15.3	4.1	0.0021	95.68
1000 ppm	-0.531	17.1	4.7	0.00053	98.91

#### 4.8.3 Polarisation measurement of 3 hrs immersed MS sample

After immersion of MS coupons in different solutions at 3 hr, polarization measurements were carried out at laboratory temperature (18 °C) at a potential window of  $\pm 350$  mV. Starting from acid solution to inhibitor 1000 ppm solution, the current density found to be decreased, it is due to the resistance of inhibitor solution toward corrosion reaction. Hence like in the as-immersed condition, the current density decrease is due to coverage of MS surface by inhibitor molecules.

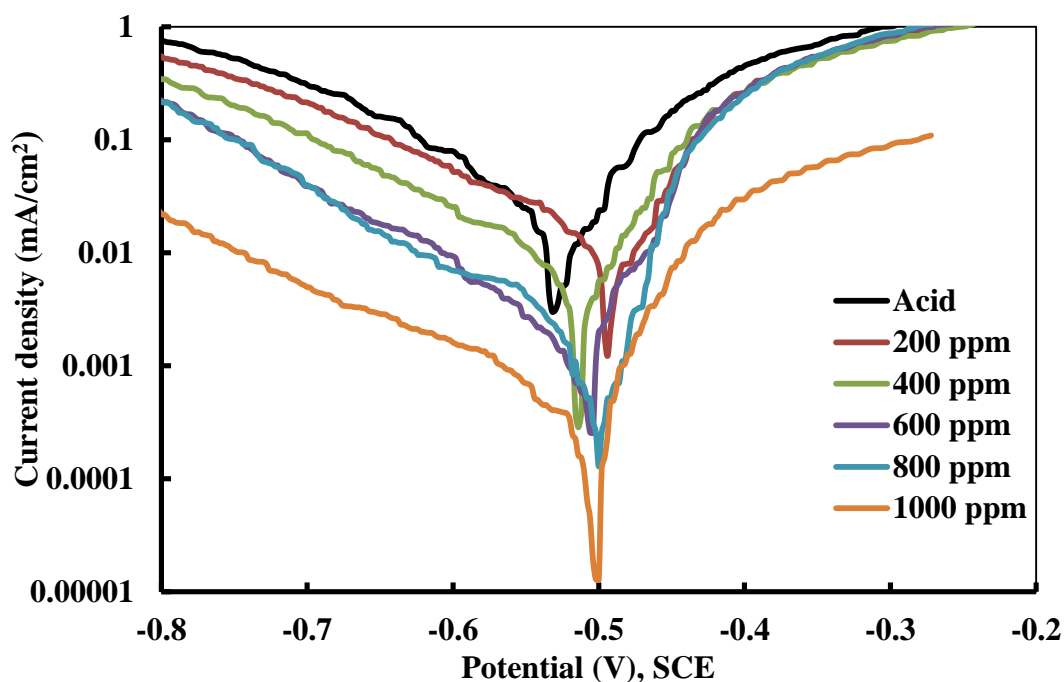


Figure 21: Potentiodynamic polarization curves for mild steel in 1M H<sub>2</sub>SO<sub>4</sub> containing different concentrations of inhibitor in 3 hr immersed condition.

The polarization curve also shows that the addition of an inhibitor causes a decrease in current density. In the presence of an inhibitor, the MS surface is covered with inhibitor molecules, resulting in a small active site. The reaction in this small area produces a small current density. This also indicates that the alkaloids used in the experiment are working as good inhibitors. The inhibition efficiency, cathodic and anodic slope, corrosion potential, and corrosion current densities of the alkaloid are also tabulated in Table 8.

*Table 8: Table showing the anodic slope, cathodic slope and inhibition efficiency for 3 hours immersed sample.*

Medium	OCP (V)	Anodic Slope (V/decade)	Cathodic Slope (V/decade)	I <sub>corr</sub> (mA/cm <sup>2</sup> )	Inhibition Efficiency (%)
Acid	-0.527	12.9	8.2	0.0205	
200 ppm	-0.497	17.1	9.3	0.0079	61.46
400 ppm	-0.508	15.9	5.8	0.0057	72.20
600 ppm	-0.514	14.3	7.3	0.0017	91.71
800 ppm	-0.502	13.9	5.1	0.0009	95.61
1000 ppm	-0.507	17.3	6.2	0.0003	98.54

In acid alone solution, the current density is 0.0205 mA/cm<sup>2</sup> and the corrosion potential is -0.527 V. The addition of varied inhibitor concentrations and polarization results in a drop in current density. At 1000 ppm inhibitor solution, the lowest current density is 0.0003 mA/cm<sup>2</sup> with a corrosion potential of -0.507 V. This drop in current density is caused by the adsorption of inhibitor molecule on the MS surface, which forms a protective barrier and reduces active sites. The anodic and cathodic slopes of each polarization curves for both as-immersed and immersed condition have not been changed. This implies that the corrosion control mechanistic pathway has not been changed.

#### **4.8.4 Inhibition efficiency from polarization measurement**

The inhibition efficacy of the inhibitor at different concentrations was assessed using the polarization technique for both immersed and as-immersed samples. The efficiency figures are shown in the tables above (Tables 7 and 8). The inhibitor's inhibition efficacy is better in As-immersed than in 3 h immersion condition. Figure 21 depicts the variance in inhibitor effectiveness with varied concentrations for mild steel in both immersed and as-immersed circumstances.

According to figure 22, it is clear that the efficiency increases with an increase in the concentration of the inhibitor. It is due to the more availability of inhibitor molecules to get adsorbed on the surface of the MS sample. The maximum efficiency was found to be 98.91 % and 98.54 % in as- immersed and 3 hr immersed MS samples respectively at 1000 ppm concentration.

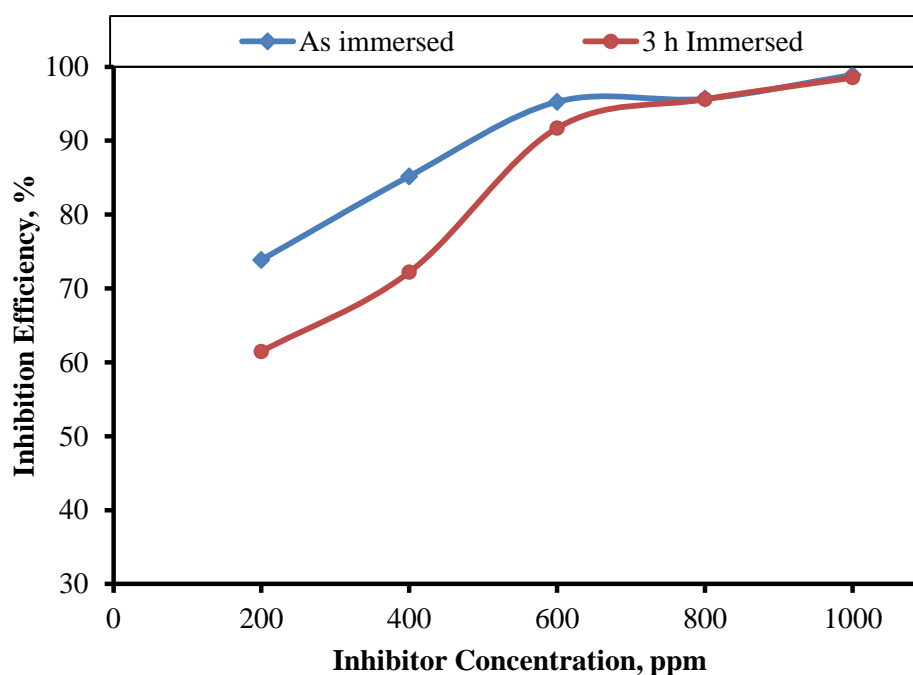
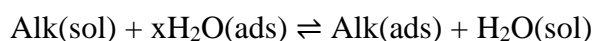


Figure 22: Inhibition efficiency of inhibitor obtained from the polarization of both immersed and as-immersed MS samples in different concentrations of inhibitor

#### 4.9 Corrosion Inhibition Mechanism

Corrosion inhibition is due to the adsorption of alkaloids on the MS surface by the replacement of water molecules.

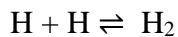
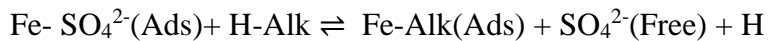
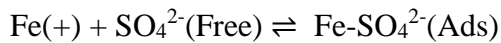


Where Alk(sol) and Alk(ads) represent the solvated and adsorbed alkaloid molecules, respectively. Similarly, H<sub>2</sub>O(ads) represents the adsorbed water molecules on the MS surface, and x represents the size ratio i.e. the number of water molecules that are replaced by one alkaloid molecule(Dhakal et al., 2022).

The OCP of the MS in corrosion cell containing aggressive media in presence and absence of inhibitor was measured. It is found that the OCP value shifted to more

positive direction in presence of inhibitor solution to acid only solution. This positive shifting of potential reveals that the MS surface is positively charged which interacts with the negatively charged sulphate ions in the medium and becomes negative. Then the negatively charged surface interacts with the protonated alkaloids electrostatically. Consequently deprotonation of alkaloids occur liberating H<sub>2</sub> gas (Karki et al., 2021). Afterwards, there may exist donor-acceptor relation between vacant d-orbital with the highest occupied molecular orbital of the alkaloids to form a coordinate bond. Here, lone pair of electrons as well as  $\pi$ -electrons of the alkaloids acts as donor and vacant d-orbital of Fe acts as acceptor (Erami et al., 2019; Qiang et al., 2018). The wavy nature of the polarization curve could be due to the increase in randomness in the solution while evolution of H<sub>2</sub>. This randomness could influence on the conductance of the electrolytic solution.

For a short while the degree of randomness increases. This is supported by transition entropy of the system. Based on the enthalpy, entropy, activation energy and OCP of the system, following may be the possible adsorption mechanism.



Where Alk(sol) and H-Alk represents the solvated and protonated alkaloids, respectively. Fe(+) and Fe-SO<sub>4</sub><sup>2-</sup>(Ads) are positively charged MS and sulphate ion adsorbed MS, respectively and Fe-Alk(Ads) is alkaloid adsorbed MS.

The polarization measurement reveals that there is decrease in current density in the presence of inhibitor for both immersed and as-immersed conditions. The inhibition efficiency of as immersed sample is nearly equal to the efficiency obtained in the polarization of immersed samples. This finding reflects that the alkaloids work from very beginning. The corrosion potential values are slightly increasing towards positive direction as the concentration of inhibitor increases. This implies that the MS surface becomes more positive as the inhibitor concentration increased. That favors the



adsorption of alkaloids on the MS surface (Erami et al., 2019). Cathodic slope of the polarization curve is found to be parallel i.e. no change in the trend of slope which indicates the hydrogen evolution is activation controlled and the reaction mechanism has not been changed up on addition of alkaloids in acid solution(Chkirate et al., 2021; Tan et al., 2021). Both anodic and cathodic slopes for in the polarization measurements has not been changed up on addition of alkaloids this indicates that the inhibition is due to adsorption of alkaloids in the MS surface entirely blocking the sites(Fekkar et al., 2020; Hafez et al., 2019).

## CHAPTER 5

### CONCLUSION

A green inhibitor for mild steel in 1M H<sub>2</sub>SO<sub>4</sub> was effectively synthesized from *Acacia catechu* bark extract in this study. The corrosion of mild steel was evaluated in the presence and absence of inhibitors using the weight loss technique and electrochemical (OCP measurement & potentiodynamic polarization) methods at various inhibitor concentrations (200 ppm, 400 ppm, 600 ppm, 800 ppm, & 1000 ppm) and temperatures. Alkaloids are effectively extracted by methanol extract utilizing the liquid-liquid extraction technique and characterized using phytochemical and spectroscopic methods during the process. The following assertions may be deduced from the data and outcomes obtained are,

- The weight loss of mild steel increased with time in both the presence and absence of inhibitor in 1M H<sub>2</sub>SO<sub>4</sub> which in turn increases the corrosion rate. However, the extent of weight loss is greatly reduced in presence of inhibitors.
- The weight loss of mild steel decreased with an increase in the concentration of the inhibitor in 1M H<sub>2</sub>SO<sub>4</sub> and so does the corrosion rate.
- The inhibition efficiency of the inhibitor seemed to increase at all immersion time as its concentration increased. The maximum inhibition efficiency of 93.96% at 1000 ppm concentration for 3 h immersion time.
- The result of the UV spectrophotometer indicates that the alkaloid extract from the bark of *A. catechu* shows the presence of unsaturated organic compounds has  $\pi$ - $\pi^*$  transition in the UV-visible region.
- FT-IR results confirmed the presence of C-N, O-H, C-O, C=O, C-H, O-H and which act as active binding sites for adsorption.
- The calculated thermodynamic parameters reveal that the adsorption process is endothermic and physical adsorption is dominated by the chemical adsorption process.
- Potentiodynamic polarization analysis showed that the *Acacia catechu* extract act as a mixed type of inhibitor for corrosion of steel in acidic solution.
- Potentiodynamic polarization analysis showed that inhibition efficiency increased with increasing the concentration of inhibitor in both cases i.e. as-immersed and immersed for 3 hours. The maximum efficiency of the as-immersed and the 3 hrs

immersed sample was found to be 98.91 and 98.54 % in the 1000 ppm of inhibitor solution respectively.

Thus, it can be concluded that the bark of *Acacia catechu* contains alkaloids which when extracted and used as a green corrosion inhibitor give efficient corrosion control to mild steel in 1M H<sub>2</sub>SO<sub>4</sub> up to 24 hours.

## References

- Arthur, D. E., Jonathan, A., Ameh, P. O., & Anya, C. (2013). A review on the assessment of polymeric materials used as corrosion inhibitor of metals and alloys. *International Journal of Industrial Chemistry*, 4(1), 2. <https://doi.org/10.1186/2228-5547-4-2>
- Chkirate, K., Azgaou, K., Elmsellem, H., El Ibrahimi, B., Sebbar, N. K., Benmessaoud, M., El Hajjaji, S., & Essassi, E. M. (2021). Corrosion inhibition potential of 2-[(5-methylpyrazol-3-yl) methyl] benzimidazole against carbon steel corrosion in 1 M HCl solution: Combining experimental and theoretical studies. *Journal of Molecular Liquids*, 321, 114750.
- Dhakal, K., Bohara, D. S., Bist, B. B., Oli, H. B., Bhattarai, D. P., Singh, S., Karki, N., & Yadav, A. P. (2022). Alkaloids extract of *Alnus nepalensis* bark as a green inhibitor for mild steel corrosion in 1 M H<sub>2</sub>SO<sub>4</sub> solution. *Journal of Nepal Chemical Society*, 43(1), 76–92. <https://doi.org/10.3126/jncs.v43i1.46999>
- Erami, R. S., Amirnasr, M., Meghdadi, S., Talebian, M., Farrokhpour, H., & Raeissi, K. (2019). Carboxamide derivatives as new corrosion inhibitors for mild steel protection in hydrochloric acid solution. *Corrosion Science*, 151, 190–197.
- Fekkar, G., Yousfi, F., Elmsellem, H., Aiboudi, M., Ramdani, M., Abdel-Rahman, I., Hammouti, B., & Bouyazza, L. (2020). Eco-friendly *Chamaerops humilis* L. fruit extract corrosion inhibitor for mild steel in 1 M HCl. *International Journal of Corrosion and Scale Inhibition*, 9(2), 446–459.
- Finšgar, M., & Jackson, J. (2014). Application of corrosion inhibitors for steels in acidic media for the oil and gas industry: A review. *Corrosion Science*, 86, 17–41. <https://doi.org/10.1016/j.corsci.2014.04.044>
- Gupta, D. K., Kafle, K. A., Das, A. K., Neupane, S., Ghimire, A., Yadav, B. D., Chaudhari, Y., Karki, N., & Yadav, A. P. (2020). Study of *Jatropha Curcas* Extract as a Corrosion Inhibitor in Acidic Medium on Mild Steel by Weight Loss and Potentiodynamic Methods. *Journal of Nepal Chemical Society*, 41(1), 87–93. <https://doi.org/10.3126/jncs.v41i1.30493>
- Hafez, B., Mokhtari, M., Elmsellem, H., & Steli, H. (2019). Environmentally friendly inhibitor of the corrosion of mild steel: Commercial oil of Eucalyptus. *International Journal of Corrosion and Scale Inhibition*, 8(3), 573–585.

- Haldhar, R., Prasad, D., & Bhardwaj, N. (2020). Experimental and Theoretical Evaluation of Acacia catechu Extract as a Natural, Economical and Effective Corrosion Inhibitor for Mild Steel in an Acidic Environment. *Journal of Bio- and Tribo-Corrosion*, 6(3), 76. <https://doi.org/10.1007/s40735-020-00368-5>
- Ijuo, G. A., Chahul, H. F., & Eneji, I. S. (2016). Kinetic and thermodynamic studies of corrosion inhibition of mild steel using Bridelia ferruginea extract in acidic environment. *Journal of Advanced Electrochemistry*, 107–112.
- Ikeuba, A. I., Okafor, P. C., Ekpe, U. J., & Ebenso, E. E. (2013). Alkaloid and Non-Alkaloid Ethanolic Extracts from Seeds of Garcinia Kola as Green Corrosion Inhibitors of Mild Steel in H<sub>2</sub>SO<sub>4</sub> Solution. *Int. J. Electrochem. Sci.*, 8, 14.
- Kamal, C., & Sethuraman, M. G. (2012). Caulerpin—A bis-Indole Alkaloid As a Green Inhibitor for the Corrosion of Mild Steel in 1 M HCl Solution from the Marine Alga Caulerpa racemosa. *Industrial & Engineering Chemistry Research*, 51(31), 10399–10407. <https://doi.org/10.1021/ie3010379>
- Karki, N., Neupane, S., Gupta, D. K., Das, A. K., Singh, S., Koju, G. M., Chaudhary, Y., & Yadav, A. P. (2021). Berberine isolated from Mahonia nepalensis as an eco-friendly and thermally stable corrosion inhibitor for mild steel in acid medium. *Arabian Journal of Chemistry*, 14(12), 103423.
- Khaled, K. F., & Hackerman, N. (2003). Investigation of the inhibitive effect of ortho-substituted anilines on corrosion of iron in 1 M HCl solutions. *Electrochimica Acta*, 48(19), 2715–2723. [https://doi.org/10.1016/S0013-4686\(03\)00318-9](https://doi.org/10.1016/S0013-4686(03)00318-9)
- Koch, G. (2017). Cost of corrosion. In *Trends in Oil and Gas Corrosion Research and Technologies* (pp. 3–30). Elsevier. <https://doi.org/10.1016/B978-0-08-101105-8.00001-2>
- Oli, H. B., Parajuli, D. L., Sharma, S., Chapagain, A., & Yadav, A. P. (2021). Adsorption Isotherm and Activation Energy of Inhibition of Alkaloids on Mild Steel Surface in Acidic Medium. *Amrit Research Journal*, 2(01), 59–67. <https://doi.org/10.3126/arj.v2i01.40738>
- Pritzl, M. D., Tabatabai, H., & Ghorbanpoor, A. (2014). Laboratory Evaluation of Select Methods of Corrosion Prevention in Reinforced Concrete Bridges. *International Journal of Concrete Structures and Materials*, 8(3), 201–212. <https://doi.org/10.1007/s40069-014-0074-3>
- Qiang, Y., Zhang, S., Tan, B., & Chen, S. (2018). Evaluation of Ginkgo leaf extract as an eco-friendly corrosion inhibitor of X70 steel in HCl solution. *Corrosion*

*Science*, 133, 6–16.

- Rahim, M. A. A., Hassan, H. B., & Khalil, M. W. (1997). Naturally Occurring Organic Substances as Corrosion Inhibitors for mild Steel in Acid Medium: Concentration and temperature effects. *Materialwissenschaft Und Werkstofftechnik*, 28(4), 198–204. <https://doi.org/10.1002/mawe.19970280410>
- Raja, P. B., Qureshi, A. K., Abdul Rahim, A., Osman, H., & Awang, K. (2013). Neolamarckia cadamba alkaloids as eco-friendly corrosion inhibitors for mild steel in 1M HCl media. *Corrosion Science*, 69, 292–301. <https://doi.org/10.1016/j.corsci.2012.11.042>
- Sayin, K., & Karakaş, D. (2013). Quantum chemical studies on the some inorganic corrosion inhibitors. *Corrosion Science*, 77, 37–45. <https://doi.org/10.1016/j.corsci.2013.07.023>
- Shrestha, P. R., Oli, H. B., Thapa, B., Chaudhary, Y., Gupta, D. K., Das, A. K., Nakarmi, K. B., Singh, S., Karki, N., & Yadav, A. P. (2019). Bark Extract of Lantana camara in 1M HCl as Green Corrosion Inhibitor for Mild Steel. *Engineering Journal*, 23(4), 205–211. <https://doi.org/10.4186/ej.2019.23.4.205>
- Sivakumar, P. R., & Srikanth, A. P. (2017). Anticorrosive Activity of Schreabera swietenioids Leaves as Green Inhibitor for Mild Steel in Acidic Solution. *Asian Journal of Chemistry*, 29(2), 274–278. <https://doi.org/10.14233/ajchem.2017.20160>
- Sunil, M. A., Sunitha, V. S., Radhakrishnan, E. K., & Jyothis, M. (2019). Immunomodulatory activities of Acacia catechu, a traditional thirst quencher of South India. *Journal of Ayurveda and Integrative Medicine*, 10(3), 185–191. <https://doi.org/10.1016/j.jaim.2017.10.010>
- Tan, B., Zhang, S., He, J., Li, W., Qiang, Y., Wang, Q., Xu, C., & Chen, S. (2021). Insight into anti-corrosion mechanism of tetrazole derivatives for X80 steel in 0.5 M H<sub>2</sub>SO<sub>4</sub> medium: Combined experimental and theoretical researches. *Journal of Molecular Liquids*, 321, 114464.
- Telegdi, J., Shaban, A., & Vastag, G. (2018). Biocorrosion—Steel. In *Encyclopedia of Interfacial Chemistry* (pp. 28–42). Elsevier. <https://doi.org/10.1016/B978-0-12-409547-2.13591-7>
- Thakur, A. V., Ambwani, S., & Kumar, T. (n.d.). Preliminary phytochemical screening and GC-MS analysis of leaf extract of Acacia catechu (L.f.) Willd.

*International Journal of Herbal Medicine*, 5.

- Thapa, B., Gupta, D. K., & Yadav, A. P. (2019). Corrosion Inhibition of Bark Extract of *Euphorbia royleana* on Mild Steel in 1M HCl. *Journal of Nepal Chemical Society*, 40, 25–29. <https://doi.org/10.3126/jncs.v40i0.27274>
- Yaro, A. S., Khadom, A. A., & Wael, R. K. (2013). Apricot juice as green corrosion inhibitor of mild steel in phosphoric acid. *Alexandria Engineering Journal*, 52(1), 129–135. <https://doi.org/10.1016/j.aej.2012.11.001>